NTNU – Trondheim
Norwegian University of
Science and Technology

Investigation of Nanoparticle Effect on Wettability and Interfacial tension

An Experimental Study of a Two-Phase
System of Heavy Oil and Di Water

Marthe Åsnes Birkeland

Petroleum Geoscience and Engineering
Submission date: June 2013
Supervisor: Ole Torsæter, IPT

Norwegian University of Science and Technology
Department of Petroleum Engineering and Applied Geophysics

Abstract

The increasing demand for hydrocarbons has led to a hope of developing more efficient recovery techniques for unconventional resources such as heavy oil. Heavy oil is movable in the reservoir, but recovery is time-consuming and expensive. Nanofluid is investigated as a possible enhanced oil recovery method. Nanofluid promise an alternation of wettability and a reduction of the interfacial tension as nanoparticles added to one of the fluid phases disturbs the initial equilibrium state.

The spontaneous imbibition test was performed to investigate how nanoparticle settlements on the pore surface influence wettability. The cores used in the tests were artificial and made of glass beads with a diameter of 1 mm where some cores where surface treated with nanofluids. The imaging method and the spinning drop method were executed to investigate how the presence and difference in hydrophilic nanoparticle concentration in di water influence the contact angle and interfacial tension. A heavy oil mixture of dodecane and bitumen was used in the experiments. The heavy oil had a viscosity of 198 cp at room temperature.

A change in rate or end volumes in the spontaneous imbibition test can be caused by altered wettability or a change in the interfacial tension between the fluids. The end volumes showed little difference between the cases. The rates obtained showed low repeatability for similar cores, but a change of rate was observed. The strongest rate change was for the hydrophobic cases. In the contact angle and interfacial tension measurements a decline was observed for the measurements with hydrophilic nanoparticles present. However, the values of both measurements increased from 0.01 wt% to 0.1 wt% of nanoparticles in the di water. The reason for this is not clear, and it contradicts the assumption of more water-wet conditions for higher nanoparticle concentrations. Besides this, the experimental results are in line with the expectations.

Sammendrag

Den økende etterspørselen etter hydrokarboner har ført til at det er ønskelig å utvikle nye effektive utvinningsstrategier for ukonvensjonelle resurser som tung olje. Tung olje har lav mobilitet i reservoaret, noe som gjør utvinningen til en dyr og tidskrevende prosess. Nanoteknologi har introdusert nanofluider til petroleumsbransjen, og det forskes på mulighetene for å utvikle nanofluid til å bli en ny metode for stimulert utvinning. Det er forventinger om at nanofluider har egenskapen til å endre fuktningsgraden og redusere grenseflatespenningen grunnet tilsatte nanopartikler i en av fluid fasene. Nanopartiklene vil forstyre den initiale likevektstilstanden.

Den spontane imbiberingstesten ble utført for å undersøke hvordan avsetning av nanopartikler på pore overflaten vil påvirke fuktegenskapene. Kjerneprøvene som ble brukt var kunstige og laget av glasskuler med diameter på 1 mm. Noen av kjerneprøvene fikk overflatebehandling med nanofluider. Bilde-metoden og snurrende dråpe -metoden ble utført for å undersøke hvordan tilstedeværelsen av ulike konsentrasjoner av hydrofile nanopartikler i den destillerte vann fasen påvirker kontaktvinkelen og grenseflatespenningen. Tung oljen som ble brukt i eksperimentene var en blanding av bitumen og dodekan. Tung oljen hadde en viskositet på 198 cp ved romtemperatur.

En endring i rate eller endevolum i den spontane imbiberingstesten indikerer en endring i fuktegenskaper eller en endring i grenseflatespenningen mellom fluidene. Endevolumet var lite forandret for de ulike tilfellene. Ratene observert viste lav repeterbarhet for like kjerneprøver, men en endring av rate ble observert. Den største endringen ble observert for de hydrofobiske prøvene. Kontaktvinkel- og grenseflatespenningsmålingene viste en nedgang i verdi når hydrofile nanopartikler var til stede i vann fasen. Men begge målingene økte når konsentrasjonen av nanopartikler økte fra 0.01 wt% til 0.1 wt%. Årsaken til dette er noe usikker, og det

motsier antagelsen om at systemet blir mer vannfuktig ved høyere konsentrasjoner av nanopartikler. Utenom dette er de eksperimentelle resultatene innenfor det forventede.

Preface

This thesis is written at the Department of Petroleum Engineering & Applied Geophysics at the Norwegian University of Science and Technology. It is the work completed in TPG 4915 Reservoir Engineering Master Thesis and was written during the spring of 2013.

The present thesis has been both educational and hectic. During the 20 weeks of my master thesis I have gained experience, and I have been challenged in the laboratory especially with unforeseen incident. The most important learning I take with me is to be patience and that laboratory work takes time. I appreciate the opportunity to get an insight in the extent of laboratory work.

I wish to thank my supervisor Professor Ole Torsæter and doctoral research fellow Shidong Li for availability and informative discussions. I would also like to thank Shindong Li, Roger Overå and Luky Hendrainingrat for introduction to the experimental instruments used in this thesis, and for help and availability in the laboratory. Last, I wish to thank to my fellow laboratory partner Anne Tinnen Kaasa for company in the laboratory, informative discussions and for general motivation throughout the process.

Trondheim, June 2013

Marthe Åsnes Birkeland

Contents

List of Figures

List of Tables

1 Introduction

The global demand of energy is expected to increase as much as 50 % for the next 20 years (Kong and Ohadi 2010). For the world to be able to meet the growing demand of energy an increase in the production of energy from both non-renewable and renewable resources is required. In the petroleum industry it is considered that most of the easy accessible oil reservoirs has been found and set on production and currently there is a decline in conventional petroleum production. To meet the future demand of petroleum the industry will either have to find new fields, increase the recovery factor of existing fields or start to produce more unconventional resources such as shale gas, shale oil, heavy oil and bitumen. About 80% of the easy accessible conventional petroleum is located in the Middle East, most of it in Saudi Arabia (Speight 2009). Though, taking heavy oil and bitumen reserves into account, America may be the future giant of petroleum assets as most of the reserves are located in Venezuela and Canada. The exploration and production of heavy oil is highly dependent on the oil price as the recovery methods used for extraction of heavy oil are expensive.

By bringing nanotechnology into the petroleum industry the hope is to develop recovery methods that are cheeper, more effective and have a better environmetal sound. Nanofluids can to develop as a recovery methods for both conventional and unconventional resources. The injection of nanoparticles as nanofluids are introduced as a possible future enhanced oil recovery method. Hydrophilic silica nanoparticles promise a decrease in the interfacial tension and a possibility of wettability alternation to strongly water-wet conditions. The motivation for investigating nanofluid for enhanced oil recovery application is development of nanofluid as a new enhanced oil recovery method. The hope is to develop an effective and less expensive recovery method for the future.

The goal of this thesis is to investigate how silica nanoparticles influence wettability and interfacial tension in a two–phase system of heavy oil and an aqueous phase (distilled water and nanofluids). The main investigations are:

- How nanoparticle settlement on the pore walls influence wettability. The hypothesis is that settlement of hydrophilic nanoparticles will make the porous media more water-wet than it was initially and generate a higher spontaneous oil production while settlement of hydrophobic nanoparticles will make the porous media less water-wet and result in a lower spontaneous oil production.
- How the difference in hydrophilic nanoparticle concentration in distilled water influence contact angle and interfacial tension. The hypothesis is that a higher concentration of hydrophilic nanoparticles distilled water will result in a decrease of the interfacial tension and an increase of the contact angle. However, a threshold can be met at higher concentrations, i.e. at a certain concentration of nanoparticles the interfacial tension or contact angle reached its minimum or maximum, respectively.

The experiments performed in this thesis will be designed and based on known and commonly used methods in the laboratory. The wettability may be quantitative defined by determining either the contact angle or the wettability index. The wettability index is obtained by the Amott method, and this method was initially planned as one of the wettability measurements. However, due to problems observed in the optimization process for the Amott method, the spontaneous imbibition test is performed instead. The spontaneous imbibition test gives qualitative results and can only indicate an alternation in wettability. For determination of the contact angle the Imaging Method is performed. Interfacial tension is measured with the use of the spinning drop method.

Chapter 2 covers the basic theory needed for the understanding of the thesis. Chapter 3 describes the experimental work performed in the laboratory. Chapter 4 shows the results and discussion of the initial optimization for the Amott method. Chapter 5 reviews the experimental results from spontaneous imbibition testing, contact angle measurements and spinning drop method are shown and evaluated. In Chapter 6 the results from the experiments will be compared to each other and some literature. The concluding remarks are given in Chapter 7.

2 Theory

This chapter is a summary of the theory relevant to the study of wettability and interfacial tension alteration by nanoparticles in a two-phase system of di water and heavy oil. The three sections explain the most important physical properties of a fluid, rock and fluid-rock interaction.

The aim of the fourth section is to emphasize the difference between heavy oil and conventional oil in the terms of geological origin, fluid properties and chemical composition.

Last, in the fifth section nanotechnology is introduced and nanofluid as a possible enhanced oil recovery method is introduced. The definition of terms like nanofluid, nanoparticle and nanotechnology is given. Propagation of nanoparticles through porous media and their wettability is covered. Also, a short review of current literature on heavy oil and nanotechnology is given.

2.1 Rock Properties

Rock properties are the physical characteristics of reservoir rocks that makes them able to store fluids and allow for fluid flow (Schlumberger 2013). The most important rock properties are porosity and permeability. The following section is based on the following literature: Torsæter and Abtahi (2003), Rosen (2011), Ursin and Zolotukhin (2000), Schlumberger (2013) and Marshak (2006) if nothing else is mentioned.

2.1.1 Porosity

Porosity, ϕ, is a measure of the storing capacity of the reservoir. Porosity is defined the ratio of the pore volume to bulk volume as:

$$\phi = \frac{V_b - V_g}{V_b} = \frac{V_p}{V_b} \tag{2.1}$$

where the bulk volume, V_b, is the sum of the pore volume, V_p, and the grain volume, V_g. Porosity is given in fraction or in percentage of the bulk volume.

Not all pores in a porous rock are connected. This causes some pore space to be sealed off and as a result, fluid flow is not possible in the total pore space. Residual porosity is the ratio of the volume of the pores that are closed off by the reservoir matrix to the bulk volume. Effective porosity is the ratio of the volume of the pores that are interconnected to the bulk volume. Effective porosity is of most importance as it reflects the volume available for fluid flow, and it is usually measured in the laboratory.

Helium porosimeter is a common method used to measure porosity of core samples in the laboratory. The experimental set-up and procedure is given in Section 3.3.1.

2.1.2 Permeability

Permeability, k, is a property of porous medium, and it is a measure of the capacity of the medium to transmit fluid. Permeability is also described as a measure for how easily (or not) a fluid flows through porous media.

Darcy's law relates the flow velocity, u, to the permeability and according to Darcy they are proportional. Darcy's law is given as follows:

$$u = \frac{k}{\mu} \cdot \frac{\Delta p}{L} \tag{2.2}$$

where Δp is the pressure difference over a distance, L, and μ is the viscosity of the fluid. The flow velocity, u, is equal to the volumetric rate, q, divided by the cross-section, A, perpendicular to the flow over the distance, L. Permeability has the SI-unit of m^2 and field units of Darcy's (D). 1 D equals $10^{-12} m^2$. Some

observations can be seen from Equation 2.2: Permeability is a tensor which is strongly dependent on pressure. Also the rate, q, is proportional to permeability and inversely proportional to the viscosity. In other words, if the viscosity of the oil is decreased or if the permeability is increased, the oil rate will increase.

There are several limitations to be considered when applying Darcy's law. It is only valid for Newtonian, incompressible fluids, no slippage between the fluid and wall, and laminar flow where the Reynolds number is less than 10.

Due to the no slippage limitation Darcy's law is not valid for gases flowing through porous media at low pressure. It is called the Klinkenberg effect. Slippage occur when the diameter of the pore approach the mean free path of the gas. To avoid slippage the diameter if the pore should be much larger than the free mean path. The mean free path of a gas is a function of pressure, temperature and the molecular weight of the gas. It is important to correct for the effect when permeability is measured in the laboratory using air or other gases at low pressure. Slippage between flowing gas and pore wall will result in apparent higher permeability.

In the present thesis a constant water rate through the core is used for measurement of permeability. The experimental set-up and procedure for this method is given in Section 3.3.2.

2.2 Fluid Properties

Fluid properties are the physical characteristics of fluids that affect their flow. The most important fluid properties are density, viscosity and interfacial tension. They are all covered in the below, and the sections are based on the following literature: Torsæter and Abtahi (2003), Ursin and Zolotukhin (2000), Rosen (2011) and Schlumberger (2013).

2.2.1 Density

Density, ρ, is defined as mass per unit volume. It is a function of temperature and pressure. Density has the SI-unit of kg/m^3.

Specific gravity (SG or γ) and API gravity are two terms used to describe the density of a fluid. For liquid, SG is defined as the ratio of density of the liquid

to density of water at the same temperature. For gases, it is the ratio of density of the gas to density of air at the same temperature. The density of water at standard conditions are 1000 kg/m^3 while for air at standard conditions it is 1.23 kg/m^3. The standard conditions in the petroleum industry for international trade of petroleum are 15°C (60°F) and 1 atm. This is different from the standards in chemistry where standard conditions are 25 °C and 1 atm.

API gravity was developed by the American petroleum institute (API). It is referred to on an API scale where most values falls within the range of 10° until 70° (Schlumberger 2013). The formula for API gravity is:

$$\text{API}^\circ = \frac{141.5}{\text{SG}_{60^\circ\text{F}}} - 131.5 \tag{2.3}$$

where SG is the specific gravity of the fluid at standard conditions.

Density does not have a direct impact on the physical flow properties such as permeability, but it usually increase with viscosity which has a high impact on the fluid flow. The density will be measured using a picknometer as described in Section 3.2.3.

2.2.2 Viscosity

Absolute or dynamic viscosity, μ, of a fluid is a measure of the internal resistance to flow. The absolute viscosity is defined as the relation between the shear stress, τ, and shear rate, γ, as follows:

$$\mu = \frac{\tau}{\gamma} \tag{2.4}$$

This equation holds only for Newtonian fluids where the shear stress is proportional to the shear rate. The unit used for viscosity is Pascal second (Pas) in SI units and centipoise (cp) in field units. One centipoise is equal to 1/100 poise and 0.001 Pas.

Kinetic viscosity, ν, is also used by the oil industry. It is defined as the dynamic viscosity divided by the density of the fluid, and the unit is centistokes (cSt).

Viscosity of fluids is a function of pressure and temperature. For most liquids, the effect of pressure can be ignored while the effect of temperature on viscosity is substantial. Temperature has different effects on the viscosity of liquids and gases. A decrease in temperature leads to an increase in the viscosity of a fluid while the opposite for gas. Viscosity also increases with molecular number.

High viscosity measurements are performed with a rotating viscometer as described in Section 3.2.4.2. Low viscosity measurements, like of water, are executed with a capillary viscometer as described in Section 3.2.4.1.

2.2.3 Surface and Interfacial Tension

Surface and interfacial tension (IFT), σ, is a property of the interface of two immiscible phases. When both of the phases are liquids, like oil and water, the term interfacial tension is used. When the phases are different, like gas and liquid, surface tension is used.

Interfacial tension is the tendency of a liquid to expose a minimum free surface when it is in contact with an immiscible fluid, and interfacial tension acts perpendicular to the interface as shown in Figure 2.1.

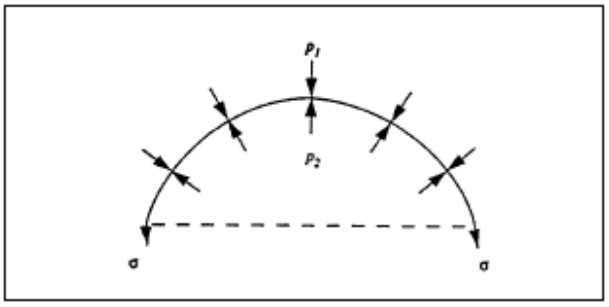

FIGURE 2.1: Interfacial tension acts perpendicular to the interface between the two immiscible fluids (Torsæter and Abtahi 2003).

The Young-Laplace equation describes the discontinuity in pressure, p_2 - p_1 , across the interface between two immiscible fluids as follows:

$$p_2 - p_1 = \sigma(\frac{1}{r_1} + \frac{1}{r_2}) \tag{2.5}$$

where r_1 and r_2 are the curvatures of the surfaces and σ is the interfacial tension between the two immiscible fluids. The discontinuity in pressure over an interface is called capillary pressure and is describes in Section 2.3.3.

Interfacial tension is measured in the present thesis with a spinning drop apparatus. The experimental set-up and procedure is described in Section 3.5.

2.3 Properties of Fluid-Rock Interaction

The most important properties of fluid-rock interaction are wettability, saturation, capillary pressure and relative permeability. These parameters describe the interaction of the fluid-rock interaction on a micro scale. The following section is based on the following literature: Torsæter and Abtahi (2003), Ursin and Zolotukhin (2000), Rosen (2011), Schulte (2012), Dake (1978) and Schlumberger (2013) if nothing else is mentioned.

2.3.1 Wettability

Wettability is a surface phenomenon where there two immiscible fluids are in contact with a solid surface. Wettability describes the interactions between fluid and rock, i.e. how the fluid(s) will tend to spread on the rock surface.

The wettability and wetting condition can be expressed through the wettability index, WI, or the contact angle which is measured through the densest fluid phase relative to the rock surface. In an oil-water system as shown in Figure 2.2, the rock surface can be described as water-wet, intermediate-wet or oil-wet. In such a system the contact angle is determined through the densest phase which in most cases is water. The values of the wettability index and contact angle and their corresponding wetting condition is shown in Table 2.1.

TABLE 2.1: Wettability index (WI) and contact angle for different wetting conditions.

Wetting Index $\cos\theta$	Contact angle θ	Wetting condition
1.0	0°	Completely water-wet
0	90°	Neutral system
-1.0	180°	Completely oil-wet

The relation between the contact angle, θ and the interfacial tension can be derived by Figure 2.2, and the relation is as follows:

$$\sigma_{\mathrm{wo}} \cdot \cos\theta = \sigma_{\mathrm{so}} - \sigma_{\mathrm{sw}} \tag{2.6}$$

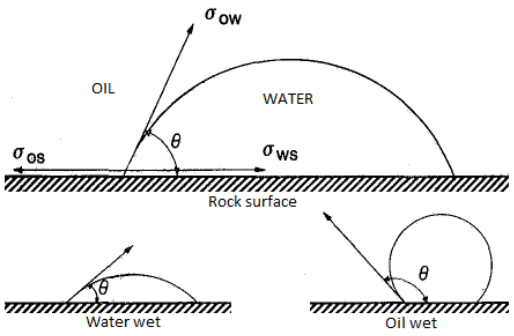

FIGURE 2.2: Illustration of interfacial tension for a two-phase system with water and oil on a rock surface (Anderson 1986).

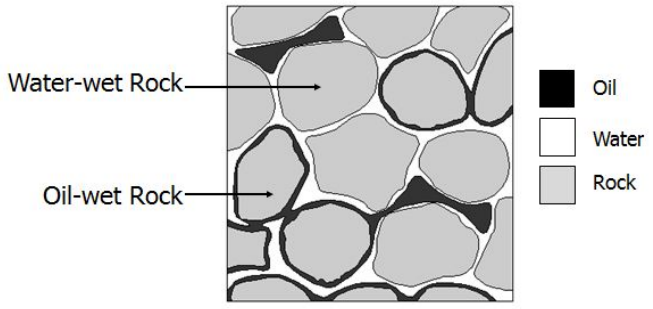

FIGURE 2.3: Illustration of a porous system of mixed wettability. Some grains are oil-wet where the oil is coating the grain while others are water-wet (Guo 2011).

where σ_{wo} is the interfacial tension between water and oil, σ_{wo} is the surface tension between solid and oil and σ_{sw} is the surface tension between solid and water.

Figure 2.3 is an illustration of a porous media where different grains have unlike wetting preference. It is referred to as a system of mixed wettability. In a water-wet system, water is coating the rock surface completely and tends to be occupying the smaller pores while oil is situated in the center of the larger pores. After water flooding residual oil is trapped as big droplets in the center of the larger pores due to the discontinuous phase. In an oil-wet system it will be the other way around. Oil is then coating the rock surface and occupying the smaller pore space while water is in the center of the larger pores. The residual oil is then the oil that is coating the rock. In a neutral system (intermediate wet) the situation in the porous media is a mix of the two described above.

Wettability is the main characteristic evaluated in the present thesis. The contact angle is measured by the Imaging method as described in Section 3.4.3, and the

relative wettability change is evaluated with the spontaneous imbibition test as described in Section 3.4.2.

2.3.2 Saturation

Saturation, S, is the relative amount of a fluid in the pore space and is expressed as follows:

$$S_\alpha = \frac{V_\alpha}{V_p} \tag{2.7}$$

where V_p is the volume of the pore space, V_α is the volume of a fluid in the pore space andα refers to the oil, water or gas phase. As porosity, saturation is given as fraction or in percentage of the pore volume. The sum of the saturation of the phases (oil, water and/or gas) present in the pore space is equal to one:

$$S_o + S_w + S_g = 1 \tag{2.8}$$

Saturation is a function of the rocks wettability and is important when it comes to how easy the fluid flows through porous media. If the fluid phase is continuously connected through the pore space then it flows more easily than a fluid that is surrounded by another phase. Droplets or 'blobs' of a phase may be trapped in the pore space when completely surrounded by another phase. When oil is displaced by water and the remaining oil no longer flows, the amount of oil left behind in the porous media is referred to as the residual oil saturation, S_{or}. When water is displaced by oil and the water no longer flows, it is called the irreducible water saturation,S_{wr}. Connate water saturation, S_{wc}, is the water saturation in the reservoir before starting production. The movable fraction of oil is: $1 - Swr - S_{or}$. The use of enhanced oil recovery techniques may reduce the residual oil saturation. This will lead to a higher recovery.

Saturation is not directly measured in present thesis, but residual oil saturation is calculated for the experiments performed on cores.

2.3.3 Capillary Pressure

Capillary pressure is the difference in pressure between two immiscible phases in the pores space, and it is given by Equation 2.9 which is the pressure in the non-wetting phase minus the pressure in the wetting phase. The pressure difference is caused by a discontinuity in pressure on the interface between the two fluids. For an oil-water system, the capillary pressure is defined as: $p_c = p_o - p_w$ where o stands for oil and w for water. Recall that the Young Laplace (Equation 2.5) gives the relation between the capillary pressure and the curvature of the interfaces. The same equation may be modifies to give the capillary pressure as follows:

$$p_c = p_{nw} - p_w = \sigma(\frac{1}{r_1} + \frac{1}{r_2}) \tag{2.9}$$

where p_{nw} is the pressure of the non-wetting phase, p_w is the pressure of the wetting phase, σ is the interfacial tension, and r_1 and r_2 is the curvature of the interfaces.

Drainage is defined as the process where the non-wetting phase is displacing the wetting phase. Imbibition is defined as the process where the wetting phase is displacing the non-wetting phase. For simplicity and to avoid confusion, imbibition in an oil-water system refers to the process where oil is displacing water even though oil is the wetting phase and drainage refers to the opposite, e.g. the process where water is displacing. This is due to the underlying assumption that all reservoirs are considered to be water-wet.

Porous media has a distribution of different pore throat sizes where the wetting fluid is occupying the smaller space and the non-wetting fluid is occupying the center in the larger space. During drainage more pressure is applied to the non-wetting phase. Gradually smaller pore throats are invaded of the non-wetting phase which leads to a decrease in the saturation of the wetting phase. Typical imbibition and drainage curves are shown in Figure 2.4. The upper-most curve is the primary drainage curve. Primary drainage is when the core is initially fully saturated with water, $S_w = 1$, and water is displaced by oil. The imbibition curve is the lower-most curve going from S_{cw} to S_{or}. The imbibition curve is found by first letting water spontaneously imbibe the core until the spontaneous water saturation, S_{spw}, is reached. After forced imbibition is performed, i.e. until no more oil is released, then S_{or} is reached. The secondary drainage curve is the curve in

the middle going from S_{or} to S_{cw}. The secondary drainage curve is found by first drain the oil spontaneously until the spontaneous oil saturation, S_{spo}. Second, forced drainage is performed until no more water is released at S_{cw}.

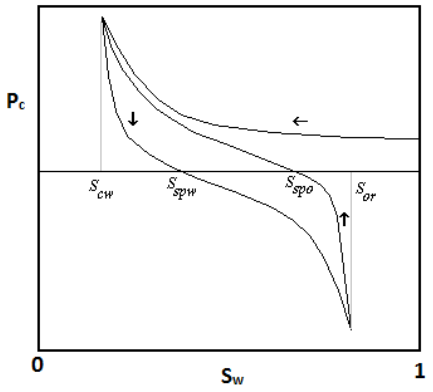

FIGURE 2.4: The capillary pressure as a function of saturation shows the drainage and imbibition curves (Torsæter and Abtahi 2003).

The capillary pressure is not measured in the present thesis. The methods used in laboratory experiments to measure the capillary pressure can be found in the literature.

The Effects of Wettability on Capillary Pressure

Wettability effects the capillary pressure together with the saturation history and the pore throat distribution (Anderson 1987a). No simple relation links the wettability to the capillary pressure curves. However, USBM, also called the centrifuge method, is an experimental method used for determination of wettability based on the correlation between the areas under the capillary pressure curves and the wetting condition. The imbibition and drainage curves are obtained only by forced imbibition and forced drainage, no spontaneous volumes or rates are considered. For a water-wet system the area under the forced drainage curve, A_1, is expected to be larger than the area under the forced imbibition curve, A_2. For an oil-wet system, A_2 is expected to be larger than A_1. While for a system of neutral wettability A_1 and A_1 are expected to be equal.

2.3.4 Effective and Relative Permeability

Effective permeability, k_e, is a measure of how easy a fluid is transmitted through porous media when another phase is present. The dimension of effective permeability is the same as for absolute permeability: Darcy, D, or m^2.

Relative permeability, k_r, describes the interaction of the phases while flowing through a porous medium as a function of the saturation. It is the ratio of effective permeability to absolute permeability as follows:

$$k_{r\alpha} = \frac{k_{e\alpha}}{k} \tag{2.10}$$

where α refers to the oil, water or gas phase.

With the use of effective and relative permeability, Darcy's law (Equation 2.2) can be modified so that the equation holds for two- or three-phase flow in porous media:

$$u_\alpha = \frac{k \cdot k_r\alpha}{\mu_\alpha} \cdot \frac{\Delta p}{L} \tag{2.11}$$

where k is the absolute permeability, μ is the viscosity and Δp is the pressure over the distance, L, and α refers to the oil, water or gas phase.

The effective and relative permeability are not measured in the present thesis. The methods used in laboratory experiments to measure the these properties can be found in the literature.

The Effects of Wettability on Relative Permeability

Wettability effects relative permeability as the wetting condition of the porous media determines the distribution of the fluids in the pores and hence the flow (Anderson 1987b). As a consequence the shape of the relative permeability curve is dependent on wettability as shown in Figure 2.5. The fluid path for the wetting fluid is often through the smaller and low permeable pores. At low saturations of the non-wetting fluid, this phase will be discontinuous through the pore space and left as droplets in the larger pores. This blocks the pore throats, and lowers

the available flow area for the continuous wetting phase. Hence, it also lowers the relative permeability of the wetting phase. As the non-wetting fluid has its fluid path in the center of the larger pores the non-wetting phase has a higher permeability at any saturation. Example, take a look at Figure 2.5: the oil relative permeability is always higher in the water-wet case, and the water relative permeability is higher in the oil-wet case. Also, at low saturation of the wetting fluid the relative permeability of the non-wetting fluid often approach the absolute permeability.

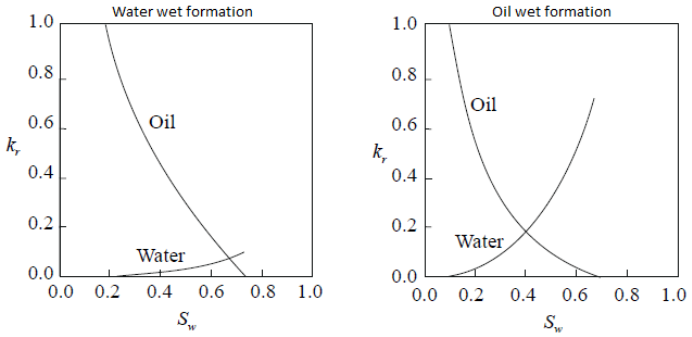

FIGURE 2.5: Visualizaion of how the wettability of the formation may affect the relative permeability curves (Ursin and Zolotukhin 2000).

2.4 Heavy Oil

The aim of the present section is to highlight the difference between conventional oil, heavy oil and bitumen. A short review over the differences in properties, geological origin and chemical composition is given. Also the most common recovery methods for heavy oil are explained shortly. If nothing else is mentioned, the present chapter is based on the following literature: van Kruijsdijk (2012), Speight (2009), Guo (2011) and Luthi (2011).

2.4.1 Classification of Hydrocarbon Reservoir Fluids

Petroleum and crude oil are equal terms and their definition is "a natural occurring mixture of hydrocarbons which may also include compounds of sulfur, nitrogen, oxygen, metals and other elements" (Speight 2009). The term conventional petroleum covers the petroleum fluids that are produced and recovered through

utilizing the easily free flow of the liquid. Unconventional petroleum is used for resources such as shale gas, shale oil, heavy oil, extra heavy oil and bitumen.

Compared to conventional petroleum, heavy oil is a crude oil with higher viscosity and higher density, i.e. lower API gravity. And according to API classifications, the term heavy oil covers crudes with an API density below 22.5° (Schlumberger 2013). Though the properties of the fluids give some impression of their characteristics the definitions of light crudes and heavy oil based on fluid properties are not absolute. An own assessment of judgment based on the fluid properties and chemical composition is necessary when labeling a reservoir fluid. The pour point of the hydrocarbon fluid is also important as the viscosity and density not always reflect this property. The pour point of a fluid is the temperature at ambient pressure where the fluid is no longer liquid like. Generally, crude oils from different geological origins have different properties.

The difference of bitumen and heavy oil can also to some extent be determined by their viscosity and density as bitumen often have higher density and higher viscosity. However, more relevant are the conditions of the fluid when in the reservoir. Bitumen is immobile in the reservoir while heavy oil is mobile, i.e. the same hydrocarbon fluid can be considered to be both bitumen and heavy oil at different reservoir temperatures. The mobility of a hydrocarbon is dependent on the pour point of the fluid and the reservoir temperature. The pour point of a fluid is the lowest temperature at which the fluid will flow.

Table 2.2 compare the fluid properties of heavy oil with the fluids used in this thesis.

TABLE 2.2: Comparison of the fluid properties of water, n-dodecane, heavy oil and bitumen as these are the fluids used in the thesis (Aylward and Findlay 2002)[1] (Guo 2011)[2].

Classification	Viscosity [cp]	Density [g/cm^3]	API	Temperature °C
Water[1]	1	1	10	25
n-Dodecane[1]	-	0.745	58	25
Heavy oil[2]	10^2 - 10^5	0.934 - 1	20 - 10	15.6
Bitumen[2]	$> 10^5$	> 1	< 10	15.6

2.4.2 Chemical Components

The most common elements in natural hydrocarbons are Carbon, Hydrogen, Nitrogen, Sulfur and Oxygen. These elements make up the main chemical components in hydrocarbons which can be divided into three groups: Paraffins, Naphthenes and Aromatics and examples of their structure are shown in Figure 2.6. Crude oils are often characterized based on the amount of the different hydrocarbon compounds.

Paraffins are n-alkanes with the general formula C_nH_{2n+2} where n from 1 to 4 are gases, n from 5 to 15 are liquids and n above 15 are wax-like solids such as paraffin waxes. Paraffins are saturated where the carbon atoms are arranged in chains by single bonds, both branched and straight. Naphthenes form a ring of carbonates saturated with hydrogen and has the general formula C_nH_n where n is 5, 6 or 7. Aromatics contain at least one carbon ring, e.g. benzene C_6H_6, where every other bond is a double and single bond. Aromatics are undersaturated and may bond with hydrogen or other elements to the unsaturated ring.

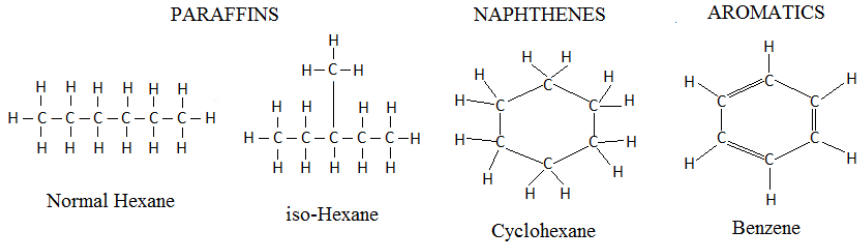

FIGURE 2.6: Examples of typical hydrocarbon components. Normal Hexane and iso-Hexane are paraffins. Cyclohexane belongs to the Napthenes, and benzene is an aromatic. Figure is free from Guo (2011).

Non-hydrocarbon compounds can include any of the three hydrocarbon components mentioned above, but are considered to be non-hydrocarbons as they contain nitrogen, sulfur or oxygen in their molecular structure. Non-hydrocarbon compounds are often found in heavier crude oils.

Resins and asphaltenes are large molecules with similar basic structure of rings, mostly aromatics. Resins dissolve in petroleum while asphaltenes are dispersed colloidal. Resins become asphaltenes by oxidation. The black color of heavy oils and bitumen compared to light oils are mainly due to presence of resins and asphaltenes.

The difference in fluid properties of light crudes and heavy oil are mainly due to their difference in chemical composition. Heavy oil is composed of a variety of both non-hydrocarbon and hydrocarbons. Like most reservoir fluids, also heavy oil varies greatly in composition. The amount of the different components in heavy oil depends on the source material of the hydrocarbon and the maturation history. Often the amount of the volatile hydrocarbons that has a lower boiling point than C_{12} is small. In general heavy oil has a lower H:C-ratio than conventional oil, i.e. it consist of long chained hydrocarbons. Heavy oil also has a higher content of carbon residues and asphaltenes, heavy metal, sulfur and nitrogen compared to conventional petroleum.

Chemical Compounds and Wettability

Denekas et al. (1959) investigated the effects of crude oil components on rock wettability. The heavier components in heavy oil can change the wettability of a reservoir when in contact with the reservoir rock for a longer period of time. Polar compounds containing nitrogen, sulfur and oxygen was found to alter wettability. Especially as the fraction of higher boiling point compounds increased the same did the effect on the sand stone wettability. The wettability was altered to less water-wet.

2.4.3 Geological Origin

Conventional oil and heavy oil are assumed to have the same origin. Five geological features have to be in place in the correct sequence for hydrocarbon to be trapped in a reservoir. These are a good source, a migration pathway, a reservoir, a trap and a seal. According to the biogenic theory, the source of hydrocarbon is sediment with a high content of biogenic decay deposited in a low-energy environment. If the biological material is buried and exposed for a certain range of temperature and pressure through geological time then hydrocarbons can be generated (biogradation). After migration from the source due to buoyancy the hydrocarbons hopefully enters a storage unit, i.e. a reservoir which is a porous and permeable rock. A trap is needed to accumulate the hydrocarbons in the reservoir. The seal prevent further upward fluid migration. The seal is often a zone with low permeability.

Heavy oil reservoirs are generally found shallow in young formations which have a less effective seal. The reservoir is typically a sandstone with good permeability and with a reservoir temperature of 40 - 60 °C. Conventional oil and heavy oil often have the same source. However, heavy oil has a less amount of light components and this can be caused by several processes:

- The heavy oil escapes the source rock before the cracking of the lighter components have occured.
- The oil escapes the source as light or medium oil and is trapped in an oxidizing zone. Processes like water washing, aerobic bacterial degradation and evaporation may then convert the oil to heavy oil.
- Biogradation has taken place in the reservoir, i.e. the reservoir is its own source.

2.4.4 Recovery of Heavy Oil

How easily a fluid flows in the reservoir can be expressed by its mobility which is a function of both fluid and rock properties. Mobility, λ of a phase is the ratio of the effective permeability to the viscosity of that phase, i.e. mobility is inversely proportional to the viscosity. The lower the mobility value the less mobile the in-situ fluid is in the reservoir. For most heavy oil reservoirs the low mobility is often the main challenge in production.

$$\lambda = \frac{\mathrm{k} \cdot \mathrm{k_r}}{\mu} \tag{2.12}$$

Heavy oil can be recovered from the reservoir by applying conventional techniques (including enhanced) oil recovery techniques. Permeability is a function of the rock which can be increased around the producing wellbore by fracturing, but it is difficult to alter the permeability in the reservoir as a whole.

Often thermal enhanced oil recovery techniques are applied to lower the high viscosity of the heavy oil and hence increase the mobility. Recall from Section 2.2.2 that viscosity of a fluid is highly dependent on temperature. Thermal enhanced oil recovery are the main applied methods to heavy oil fields where thermal energy is introduced to the reservoir often through steam injection or in-situ combustion

(injection of air that combust). The main objective is to increase the temperature of the oil so the viscosity is decrease and the mobility increase.

As mentioned in Section 2.3.4, the relative permeability is a function of the fluid distribution which is controlled by the wettability. An alternation of the wettability can therefore influence the relative permeability and lead to a better mobility for the heavy oil.

2.5 Nanotechnology as Enhanced Oil Recovery

Nanotechnology may have the solution to several challenges faced by the oil industry today, and it ranges from finding the oil, drilling wells for production, the extraction process through field life and the process facilities and transport. To get a good understanding of the new opportunities brought by nanotechnology and nanoscience, their definitions should be stated. However, the definition of nanotechnology and nanoscience is not clear in the literature. The Royal Society & The Royal Academy of Engineering (2004) did an examination on the widespread definition in the literature where the aim was to get a general definition of them both. They concluded with the following:

"Nanoscience is the study of phenomena and manipulation of materials at atomic, molecular and macromolecular scales, where properties differ significantly from those at a larger scale."

"Nanotechnologies are the design, characterization, production and application of structures, devices and systems by controlling shape and size of nanometer scale."

From the above definitions it follows that the main difference is the level of scale. Traditionally the study of phenomena in science has been done on a macroscopic level, and the observed features have been explained by properties on the same scale such as density, viscosity, etc. These are macroscopic properties of a fluid and they explain little how the atoms behave on a molecular level (Evdokimov et al. 2006). The interest area in the nanoscience is described on a scale ranging from the level of an atom (0.2 nanometer) to 100 nm where ($1\text{nm} = 10^{-9}m$) (Enderby and et al. 2004). Figure 2.7 relates some known examples to the level of nanoscience and nanotechnology.

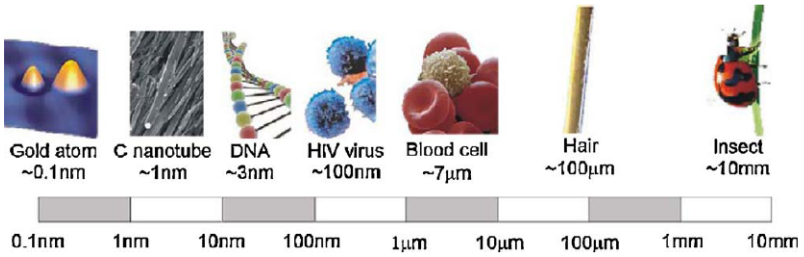

FIGURE 2.7: Visualization of the level of nanoscale. Relates some known examples to the tiny length scale (Serrano et al. 2009).

Nanotechnology opens for the possibility that in the future the reservoir engineer might simply describe to nanotechnologist what they want to measure in the reservoir, and he will develop the accurate nanotechnology that may generate the requested data. This is a simplified description to how nanotechnology may open many doors when it comes to reservoir monitoring and characterization (Hardage 2009). It is also expected that it will lead to methods which are more efficient, less expensive, and more environmental sound (Kong and Ohadi 2010). One obvious challenge is that the nanodevice has to be less than the smallest pore throats to be able to penetrate the reservoir. A comparison between the size of the nanodevice and the pore throat distribution is therefore helpful (Hardage 2009).

2.5.1 Nanoparticles

In line with the previous definition of nanotechnology and nanoscience, the Royal Society & The Royal Academy of Engineering (2004) have also given a definition on nanoparticles:

"Nanoparticles are (in most cases) defined as particles of less than 100 nm in diameter that exhibit new or enhanced size–dependent properties compared with larger particles of the same material."

Further in this report, the term nanoparticles will refer to nano-sized silica particles used for enhanced oil recovery purposes. Silica, or silicon dioxide which is the chemical name, consists of two oxygen atoms and one silicon atom and has the chemical formula SiO_2. It is an inorganic, non-crystalline solid. One of the main properties of silica is its hardness. The key factor that makes silica particles interesting for enhanced oil recovery purposes is that the wettability and other

properties of the silica particles is determined by the choice of surface coating (Zhang et al. 2010).

2.5.2 Nanofluids

A nanofluid, by some authors Saidur et al. (2010) referred to as a smart fluid, is a base fluid with nano-sized particles in colloidal suspension (Moon 2010). Nanofluids are two phase systems with one phase in another. In this report nanofluid refers to nano-sized silica particles dispersed in water as base fluid. This is a two phase system with a solid phase in a liquid phase, and an important issue is the stability of the nanoparticles in suspension. The stability problem may be solved to a certain degree by very tiny silica particles (which are immune to gravity effects). Two-step method is the most widely used methods for preparing nanofluids (Yu and Xie 2011). First, silica particles are produced as dry powders by chemical or physical crushing. Secondly, the powder is dispersed in the base fluid by mixing methods.

The stability of nanoparticles in suspension is determined by the sum of the attractive (and repulsive) van der Waals forces between the particles, and they tend to follow a random path by Brownian motion (Moon 2010). If the particles repulsive forces exceeds the attractive forces, the suspensions will be stable and aggregation is avoided (Yu and Xie 2011).

Nanofluids have a high surface-to-volume ratio which leads to superior thermal properties, and their surface-to-volume ratio may be 1000 times greater than of micro particles (Kong and Ohadi 2010). Base fluids such as water have low thermal conductivity and this can be improved by adding suspending small solid particles. By adding nanoparticles in base fluids not only the transport properties and the flow behavior is changes, but also the heat transfer ability is improved (Li et al. 2009).

2.5.3 Nanoparticle Propagation Through Porous Media

For nanofluid to be a successful enhanced oil recovery method when applied at field scale, the nanoparticles have to be able to travel long distances in the porous reservoir. The space between injector and producers is substantially larger than

the length of a core plug for which must laboratory experiments are performed. As nanofluid propagates porous media several mechanisms result in a decrease in the dispersed silica concentration (Caldelas et al. 2011). The main limiting causes of retention of nanoparticles in porous media is adhering on the pore walls and blocking of pore throats. Blocking of pore throats can be caused by two mechanisms: Mechanical entrapment and Log-jamming (accumulation) (Skauge et al. 2010).

Mechanical entrapment, also called straining, is blockage due to a larger diameter of the nanoparticle than the pore throats it is blocking. Thus silica particles are not able to penetrate the pore channel, i.e. blocking due to $d_{particle} > d_{pore\,throat}$). To avoid this effect the diameter of the nanoparticles must be smaller than the diameter of the pore throat.

Log–jamming is blockage of pore throats that are larger than each nanoparticle, i.e. the same mechanism as mechanical entrapment, but it is more complex. Pore throats can be thought of as bottlenecks in the pore channels. The narrowing of flow area and constant differential pressure will lead to a velocity increase of the fluid at the pore throat. The small H_2O molecules will accelerate faster than the nanoparticle leading to accumulation of nanoparticles at the entrance of the pore throats. First the diameter is reduced and eventually blockade occurs. Log–jamming is primarily governed by the concentration of nanoparticles, flow rate and the diameters of the pore throats (the pore size distribution).

Absorption on the rock surface may change the wettability of the rock as discussed in Section 2.5.4. However, absorption of silica particle concentration on the rock surface may lead to a decrease in silica particle concentration as the nanofluid propagates the reservoir. Adhering and detaching on pore walls is mainly controlled by the van der Waals attraction between the silica particle and the pore wall (Caldelas et al. 2011). Van der Waals forces are the forces that attract atoms and molecules together. They are universal, meaning that all molecules and atoms attract each other by this mechanism. Even when molecules and atoms are relatively far apart the van der Waals forces is significant. This is what causes the attractive forces between two nanoparticles or a nanoparticle and the pore wall. The van der Waals forces are the governing effect in adhesion and in the stability of nanoparticles in suspension (Parsegian 2006).

Caldelas et al. (2011) investigated how different factors influenced the nanoparticle propagation through unconsolidated porous media. The factors investigated were specific surface area of the porous media, lithology, brine salinity, interstitial velocity, residence time, column length and temperature effects. They used silica particles both with and without surface coating. They concluded that nanoparticle transport across distances of several meters is possible. Due to van der Walls forces the available surface area of the porous media has the highest effect on retention. It also showed that an increase in salinity of the base fluid (and the pre- and post-flush) increased the particle retention as well as the nanoparticle arrival time. The investigated temperature effect was barely noticeable.

2.5.4 Wettability of Nanoparticles

Smart fluids open for detailed control of benefits such as wettability alternation and reduction of the interfacial between oil and water. As mentioned in the previous section, the wettability of silica particles is determined by the choice of surface coating (Zhang et al. 2010). It can be made hydrophilic (hydros is Greek for water and philia for love) or hydrophobic (phobos is Greek for fear). Hydrophilic silica particles prefer to stay in the water phase. While hydrophobic is repelled from water and prefer the oil phase. The wettability of the nanoparticle determines how it will be situated on the water-oil interface. Also absorption of nanoparticles on the solid rock surface may cause a wettability change. The purpose of wettability alternation is to make the immobile oil flow. Wetting behavior of liquid changes when the liquid contains nanoparticles (Chaudhury 2003).

Zhang et al. (2010) found that hydrophilic nanoparticles produce in oil-water (o/w) emulsions, while hydrophobic nanoparticles yield water-in-oil (w/o) emulsions, i.e. the wettability of the nanoparticle determines the emulsion formed. For both o/w and w/o emulsions, higher weight percentage of nanoparticles gave an increase in the dispersed phase volume fraction and the average droplet size decreased.

Figure 2.8 illustrates how nanoparticles is situated on the interface dependent on their wettability. As discussed in Section 2.3.1, a contact angle of 90 degrease is considered intermediate wet and the nanoparticle will then ideally have 50 % surface area covered with oil and 50 % with water. A contact angle of less than 90 degrees is water-wet and a larger fraction of the surface area of the nanoparticle is then covered with water than oil. A contact angle of more than 90 degrees

is oil-wet, and a smaller fraction of the surface area of the nanoparticle is then covered with water than oil. Recall that the contact angle is determined by the densest liquid phase.

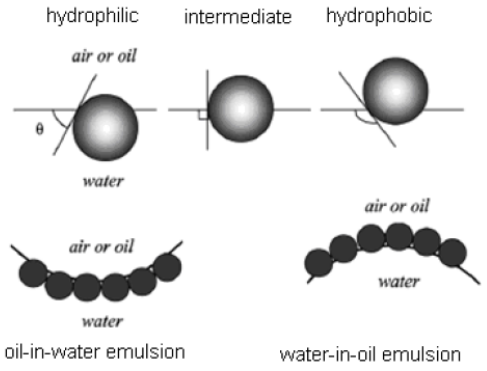

FIGURE 2.8: Contact angle of hydrophilic, intermediate and hydrophobic silica particles in different emulsions (Zhang et al. 2010).

Figure 2.9 illustrates that nanoparticles will self-assemble at the interface between the oil and the pore wall forming a thin film called a wedge layer. The oil droplet is separated from the rock due to disjoining pressure created by the wedge film which exerts a pressure on the discontinuous phase (Moon 2010). The disjoint pressure effect is a surface energy effect due to the millions of nanoparticles settled at the interface.

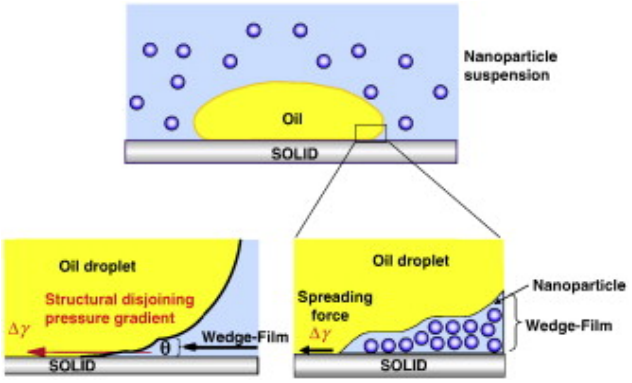

FIGURE 2.9: Illustration of how an oil droplet is loosened from the rock surface by hydrophilic silica particles (Wasan et al. 2011).

3 Experimental Work

The aim of this chapter is to give an overview of the experimental work executed. All experiments were performed at the student lab at IPT, NTNU. The experimental theory, setup and procedure in the present chapter is based on experience from the laboratory work and Torsæter and Abtahi (2003) if nothing else is mentioned. Figure 3.1 is an overview of the laboratory work. It is given to help the reader understand the sequence of the laboratory work and the preparation needed for each experiment.

The main goal of the experiments is to have a look at how nanofluids affect the wettability and interfacial tension of a two-phase system of heavy oil and an aqueous phase, di water and hydrophilic nanofluids. Two experiments are prepared for wettability; the imaging method for measurement of the contact angle, θ, and the spontaneous imbibition test for investigation of relative wettability. One experiment is prepared for the interfacial tension; the spinning drop method. Initially the Amott method was intended for wettability determination, but the method was later reduced to spontaneous imbibition testing. This is discussed in Chapter 4.

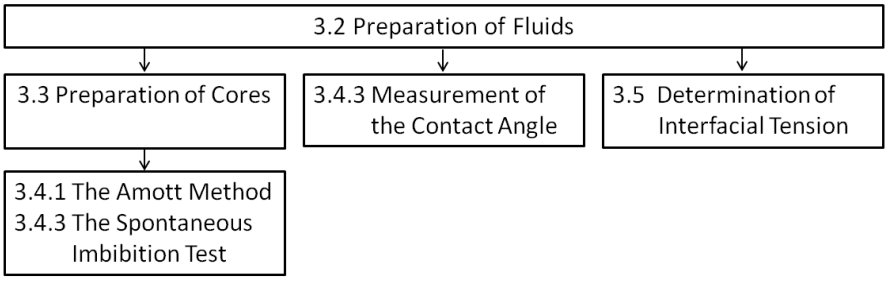

FIGURE 3.1: Overview of the laboratory work perform and the sequence at which they are executed. The purpose of the overview is to provide an understanding of the sections in the present chapter. The numbers in the boxes refer to the Section numbers.

3.1 Experimental Materials

A short summary of the materials used in the experiments is given in the following section. A full overview of fluid and solid properties can be found in Appendix A.

Nanoparticles

The silica nanoparticles were used to make nanofluids and it is their effect on the contact angle and interfacial tension that is investigated. In the experiments both hydrophilic and hydrophobic particles with the same primary particle size was used. The silica nanoparticles chosen for the experiments had an average primary particle size of 16 nm. Two types used were: Hydrophilic (AEROSIL 130) and hydrophobic (AEROSIL 130 S). The hydrophilic nanoparticles are dispersed in distilled water while the hydrophobic nanoparticles are dispersed in ethanol. This is due to their surface coating and preference towards water. The hydrophilic nanofluids are used in all experiments while the hydrophobic nanofluids are only used in the Spontaneous Imbibition Method.

Distilled water

Distilled and deionized water, di water, was used as the base fluid for hydrophilic nanoparticles. Di water is also used for the reference cases in the measurements of contact angle, interfacial tension and in the Amott cells. Di water is water where many of the impurities in regular water are removed through distillation. Distillation involves boiling of the water and condensing the steam into a clean container. The viscosity and density will be measured at room temperature (21 - 22 °C).

Ethanol

Ethanol was used as the base fluid for hydrophobic nanoparticles. The most important property to be aware of is the boiling temperature at atmospheric pressure which is 78.3°C (Aylward and Findlay 2002).

(n-)Dodecane

Dodecane was used to mix the heavy oil used in the experiments. The density of dodecane is 0.745 kg/m^3 at 25°C. The boiling temperature at atmospheric pressure is 216.3 °C (Aylward and Findlay 2002).

Bitumen

The bitumen was used to mix the heavy oil used in the experiments. The bitumen

is from Athabasca, Canada. An investigation of its chemical composition and measurement the fluid properties have been executed by Ashrafi et al. (2011), and the results can be found in their paper.

Glass bead

The glass beads were used to make artificial cores. Glass beads of several sizes were tried out. These are: 300 - 400 μm, 425 - 600 μm, 1 mm and 2 mm. The different size of glass beads gave cores with different pore throats and pore space due to sorting and their dimension.

3.2 Preparation of Fluids

The fluids prepared for the experiments are heavy oil and nanofluids. As mentioned in Section 2.2, viscosity and density are the most important parameters of fluids. They are needed as input parameters for the experiments that determine the contact angle and interfacial tension. The density of heavy oil and nanofluids are measured using a picknometer. The viscosity of heavy oil and nanofluids are measured using a rotometer and capillary viscometer, respectively.

3.2.1 Heavy Oil

The heavy oil mixture used in the experiments is a mixture of dodecane and bitumen from Athabasca, Canada. The equipment needed for mixing is shown in Figure 3.2. Preheating of the bitumen lowers the viscosity and makes it easier to handle. Also dodecane was heated, but not to the same temperature as it has a lower boiling temperature at atmospheric pressure. Different weight percentages of the two were tried out. The correct weight percentages of bitumen and dodecane to achieve the aimed viscosities of 100 cp and 200 cp at room temperature (approximately 22.5 °C) was obtained through trial-and-error and the results are shown in Section 4.1.

3.2.2 Nanofluids

For each nanoparticle type, three nanofluids are prepared with different weight percentages (wt %) of silica particles in their base fluid. These are: 0.01 wt %, 0.1

FIGURE 3.2: The equipment needed for mixing of heavy oil. From the left: a weight scale, dodecane and beaker with Athabasca bitumen and a beaker with a stirring magnet on top of the heating/stirring device.

wt % and 0.5 wt %. A normal scale was used to obtain the right amount of base fluid into a beaker while the correct amount of nanoparticles where found using an ultra-fine scale with six decimals. The nanoparticles are mixed into the base fluid using hand-held ultrasonic stirring processor. In Figure 3.3 the equipment needed for nanofluid mixing is shown. Hydrophilic nanoparticles dispersed in di water are referred to as hydrophilic nanofluid. Hydrophobic nanoparticles dispersed in ethanol are referred to as hydrophobic nanofluids.

FIGURE 3.3: The equipment needed for mixing of nanofluids. From the left: basefluid and box with nanoparticles, in this case Ethanol and AEROSIL 130 S, a weight scale with beaker and the ultrasonic processor.

3.2.3 Density Measurement

Density was determined with the use of a pycnometer which is a small flask with a known volume and a stopper. The weight of the fluid was obtained by weighting the pycknometer before and after filling of the flask. The density, ρ, of the fluids were calculated as follows:

$$\rho = \frac{\mathrm{w}}{\mathrm{V}} \tag{3.1}$$

where w is the weight of the fluid in the pycnometer and V is the volume of the picnometer.

3.2.4 Viscosity Measurements

Two methods are used for measurement of the viscosities due to the different viscosities of the heavy oil and nanofluids. The two methods are the capillary viscometer and the rotating viscometer.

3.2.4.1 Capillary Viscometer

A capillary viscometer, as shown in Figure 3.4, was used for measurement of the di water and nanofluid viscosity. Calculation of viscosity with the use of a capillary viscometer is based on Poiseuille's law:

$$\mu = \frac{\pi r^4 \rho g t}{8V} = k\rho t \tag{3.2}$$

where r is the radius of the capillary tube, ρ is the density of the fluid, g is gravity coefficient, t is the time through the capillary tube and V is the volume of the capillary tube. The radius, gravity and volume form a constant, k, which is determined by using a fluid with a known viscosity. The two constants for the capillary viscometer used are: $k_1 = 0.001980$ mm^2/s^2 and $k_2 = 0.001635$ mm^2/s^2.

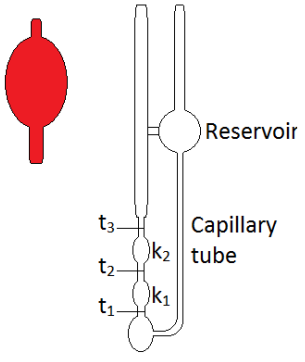

FIGURE 3.4: The balloon pump to the left is for filling of the reservoir in the capillary viscometer. t_1, t_2 and t_3 are the reference marks where the time is noted. k_1 and k_2 are constants for calculation of viscosity for separate time intervals. Viscosity is averaged over these results.

The reservoir of the viscometer was filled using a balloon pump. The time was noted at each reference mark,t_1, t_2 and t_3, with the use of a stop watch. The

viscosity was calculated by Equation 3.2 for both time intervals. The average was taken to get one value of viscosity for each fluid. The results are shown in Section 5.1.

3.2.4.2 Rotating Viscometer

The apparatus used for measuring the viscosity of heavy oil was a rotating viscometer called BROOKFIELD LVDV II Pro Viscometer. The setup is shown in Figure 3.5. The heavy oil was poured into the small cylinder and placed in the termosel. The viscosity was measured at room temperature and at an elevated temperature of 60°C as this was the temperature used in the interfacial tension measurement and for the spontaneous imbibition testing. SC4-34 and SC4-31 were the needles used in the experiments. SC4-34 was used for viscosities in the range of 250 - 36 cp while SC4-31 was used for viscosities in the range of 27.2 - 16.9 cp. The RPM of the apparatus is 40 - 200. Final step of the measurement was to choose the correct rpm and wait for the viscosity measurement to stabilize.

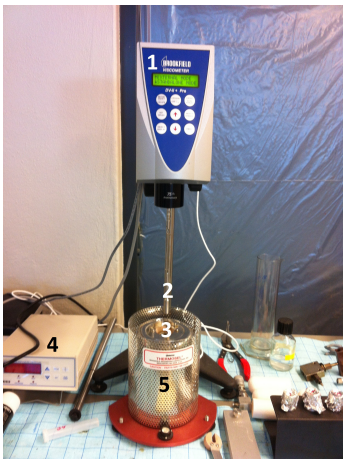

FIGURE 3.5: Setup of the rotating viscometer. 1: the main part of the rotometer. 2: the needle. 3: where the small cylinder with heavy oil is placed. 4: controlling panel for the temperature of the thermosel. 5: the thermosel.

3.3 Preparation of Cores

The artificial cores used in the experiments are made of uniform glass beads in a core holder. The dimensions of the core holder used is shown in Figure 3.6. The dimension of the glass beads will be determined by trials. The final decision is

shown in Section 4.3. At least two cores are prepared for each nanofluid and di water, so 14 cores are prepared in total. The core holder was filled with a small volume of glass beads at a time with the use of a funnel to avoid losses of beads. A shaker was used between each filling to obtain optimal packing of the glass beads. Filters were used at both ends of the core holder to avoid glass beads escaping through the inlets at each end of the core holder.

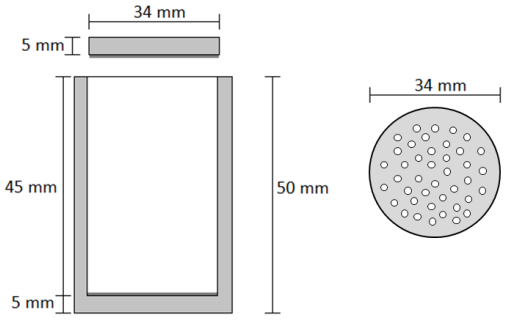

FIGURE 3.6: Sketch of the core holder with dimensions. Light grey area is the walls, lid and bottom of the core holder. The darker gray indicates filters at each end. To the right is a sketch of the inlets. Each end are filled with several holes to allow for fluid flow out and in of the core.

Surface treatment of glass beads was carried out by submerging the beads in nanofluid for 5 days to allow for settlement of nanoparticles on the surface area. After the treatment, the nanofluid was poured out, and the glass beads were dried in an oven for two days.

The porosity is measured on every core with the use of a Helium Porosimeter. Permeability is only measured on the artificial cores made of glass beads without surface treatment as the permeability measurement had to be done by using water. This is because the permeability is too high for air permeability measurement as the flow through the core is turbulent and unstable. For the surface treated cores the nanoparticles may be washed away by streaming water through the core. As the glass beads are uniform in size and neither porosity nor permeability of the cores should vary.

3.3.1 Porosity Measurement

The porosity of the artificial cores was measured with the Helium Porosimeter apparatus. It is applicable as the bulk volume, the volume inside the holder, is

known. The Helium Porosimeter apparatus measures the empty space inside the cell. The Helium porosimeter is based on Boyle's law which is as follows:

$$p_1V_1 + p_2V_2 = p(V_1 + V_2) \tag{3.3}$$

which relates the pressures in the two chambers, p_1 and p_2, with the known reference volume, V_1, the average pressure after the value between the chambers are opened, p, and the unknown volume of chamber 2, V_2, with the core inside. The setup is shown in Figure 3.7.

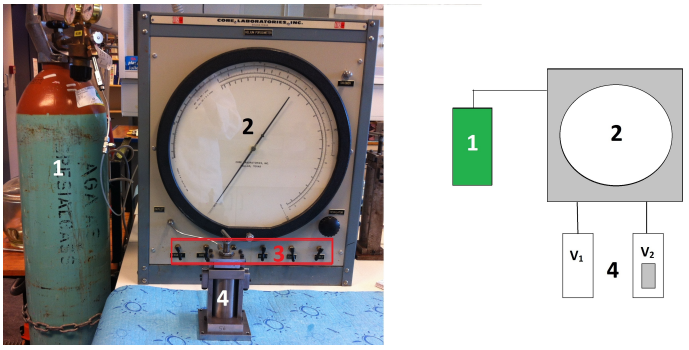

FIGURE 3.7: Picture and sketch of Helium porosity apparatus. 1: Helium supply. 2: Manometer (gives volume in cm^3). 3: Button control for opening and closure of valves. 4: Chamber. V_1 is the reference volume i.e. volume of empty chamber. V_2 is the volume of chamber minus core holder and glass beads volume.

The reference volume, V_1, the volume of the chamber with only core holder, V_{ch2}, and the volume of the chamber with artificial core, V_2, are recorded with the porosimeter. The reference volume is the volume of an empty chamber

The volume of the core holder, V_{ch}, is the reference volume subtracted by the volume of the chamber with core holder: $V_{ch} = V_1 - V_{ch2}$. The volume of the core holder has to be known as it should not be taken into account as a part of the grains. The grain volume, V_g, is obtained by taking subtracting the reference volume with the volume of the chamber with artificial core and the volume of the core holder as:

$$V_g = V_1 - V_2 - V_{ch} \tag{3.4}$$

To calculate the bulk volume the inner radius and length has to be known for the core holder. The bulk volume can be calculated as:

$$V_b = \pi \frac{d}{2}^2 L \tag{3.5}$$

And last, the porosity can be calculated as:

$$\phi = \frac{V_b - V_g}{V_b} \tag{3.6}$$

3.3.2 Permeability Measurement

The permeability determination was done by keeping the flow rate, q, through the core constant by the use of a pump and the pressure drop over the core was measured. An illustration of the setup is shown in Figure 3.8. The core was placed in a Hassler type core holder with a sleeve which prevents any flow around the core and therefore forces the water to flow through the core. The rate was set to a constant value at the pump. The rate was checked by timing the water volume out of the system.

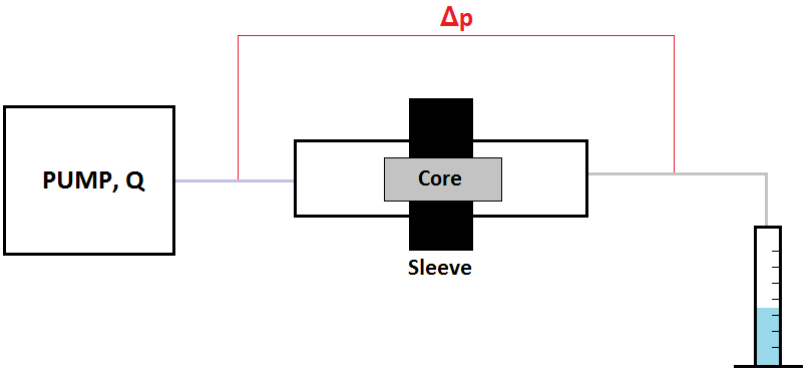

FIGURE 3.8: Illustration of the experimental setup for the permeability measurement. The core is placed in the sleeve which is a Hassler type core holder. The pump provides a constant rate of water and the pressure drop over the core is recorded by the computer. The water flowing out of the system is collected in a cylinder with a volume scale.

When the rate and pressure drop are measured, the permeability can be calculated as:

$$k = \frac{\mu L}{A} \cdot \frac{q}{\Delta p} \tag{3.7}$$

where L is the length of the core, A is the surface are of the core perpendicular to the flow rate and μ is the viscosity of water.

3.3.3 Saturation of Cores

The cores were saturated using a vacuum pump. The cores were fully saturated with one fluid, either di water or heavy oil. The setup for the use of a vacuum pump is shown in Figure 3.9. First, the cores were placed in a beaker inside the vacuum tank and the edges of the tank were sealed off with silicon. Second, the tank was vacuumed using a vacuum pump. The pressure gauge, reading the pressure inside the tank, should reach 100 mbar. Third, the fluid holder with a tube was filled with either di water or heavy oil. When heavy oil was the saturating fluid, it was heated in advance to make it less viscous. Fourth, the di water or heavy oil was poured into the beaker with cores through the tube on the fluid holder. The beaker was filled with a substantial amount of fluid covering the core. It was left for one hour to let the core fully saturate.

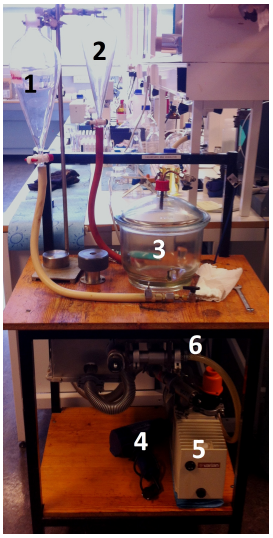

FIGURE 3.9: Picture of the vacuum pump available in the student lab. 1: Fluid holder with tube for water. 2: Fluid holder with tube for oil. 3: Vacuum tank. 4: Heater. 5: Vacuum pump. 6: Pressure gauge.

3.4 Wettability Determination

Two quantitative methods were first considered for wettability determination. These were the measurement of contact angle and the Amott method. Due to issues experienced during the optimization process of the Amott test, as discussed in Chapter 4, the Amott method was abandoned and replaced by a spontaneous imbibition test. The Amott method will be reviewed while the main focus will be

on the contact angle and the imbibition test. The contact angle is measured with the Imaging method. The spontaneous imbibition test is a qualitative method where the rates of the imbibition are compared.

3.4.1 The Amott Method

The Amott Method is an empirical method based on spontaneous imbibition and drainage with the use of Amott cells shown in Figure 3.10 and forced imbibition and drainage by for example a centrifuge.

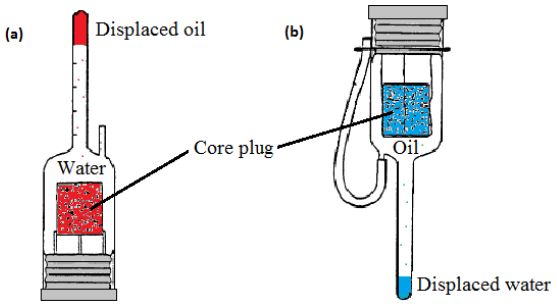

FIGURE 3.10: Figure (a) is an Amott cell with a core saturated with oil and surrounded by water. The spontaneous oil volume is recorded. Figure (b) is an Amott cell with a core saturated with water and surrounded by oil. The spontaneous water volume is recorded. Figure is free from Torsæter and Abtahi (2003) and Glover (2011).

Both oil and water spontaneous and forced production volumes are noted during the measurements. When these are known the displacement-by-oil ratio, r_w, and displacement-by-water ratio, r_o, can be calculated as:

$$r_w = \frac{\text{Spontaneous Water Imbibition}}{\text{Total Water Imbibition}} = \frac{V_{o1}}{V_{o1} + V_{o2}} \tag{3.8a}$$

$$r_o = \frac{\text{Spontaneous Oil Imbibition}}{\text{Total Oil Imbibition}} = \frac{V_{w1}}{V_{w1} + V_{w2}} \tag{3.8b}$$

where V_{O1} is the volume produced oil during spontaneous imbibition, V_{O2} is the volume of oil produces during water flooding, V_{W1} is the water produced during oil spontaneous "imbibition" and V_{W2} is the volume of water produced during oil flooding. The wettability of the core can be determined quantitative with the wettability index, WI, which can be calculated as: $WI = r_w - r_o$. The wettability index will be a number between -1 and 1 where 1 is strongly water-wet, -1 is strongly oil-wet and 0 is neutral wettability.

3.4.2 The Spontaneous Imbibition Test

In the spontaneous imbibition test the wettability of a core is determined by comparing the rate to a reference case, i.e. the spontaneous imbibition test provides an estimate on relative wettability or an alternation of wettability. The reference case in the experiment performed in this thesis was an artificial core with non-surface treated glass beads. The imbibition rate from the non-treated core represents initial wettability, i.e. the reference wettability. The spontaneous oil rate out of the cores in the Amott cells at 60°C was noted.

Figure 3.11 present the line of action for the spontaneous imbibition test. Before starting the spontaneous imbibition test, the fluids and cores has to be prepared. The procedure for fluid preparation is described in Section 3.2 and for cores in Section 3.3.

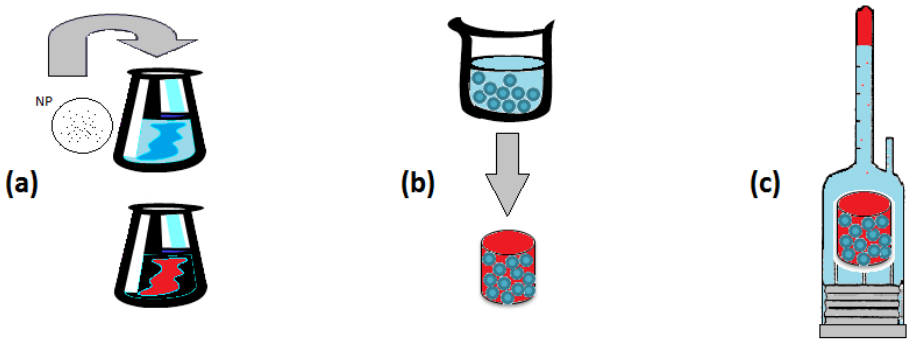

FIGURE 3.11: Schematic drawing of the line of action of the laboratory work that was done for the spontaneous imbibition test. (a) Preparation of cores. (b) Preparation of cores. (c) The spontaneous imbibition test.

Before the artificial core saturated with heavy oil was put into an Amott cell with di water, the beaker with the saturated cores, di water and Amott cell was heated to 60°C. First the Amott cell was filled with di water. Second the artificial core was inserted as shown in Figure 3.11 (c). The excess oil was dried of before the core was submerged. Third the end piece was fastened at the end of the Amott cell. The Amott cell was put into an oven at 60°C and the oil rate was noted. The Amott cell was left in the oven until no more oil was recorded.

The artificial cores with surface treated glass beads are expected to differ in rate compared to the base case. Hydrophobic cores are artificial cores made of glass beads surface treated by hydrophobic nanofluids. While hydrophilic cores are artificial cores made of glass beads surface treated by hydrophilic nanofluids. The

hydrophobic cores are expected to have lower imbibition rates while the hydrophilic cores are expected to have higher imbibition rates. Also the higher the concentration of nanoparticles, the higher change of rate is expected. Lower imbibition rates indicate a more oil-wet core. Higher imbibition rates indicate a more water-wet core.

3.4.3 Measurement of the Contact Angle

The contact angle, θ, of heavy oil and a water phase (nanofluid or di water) was measured using the imaging method. The imaging method is based on Young's law (Equation 2.6). The contact angle is measured through the denser phase which in this case was the aqueous phase. Figure 3.12 include three examples of how a droplet of oil on a solid can behave when in contact with a water phase. Table 2.1 shows for which contact angles the system is considered water-wet, intermediate-wet or oil-wet. The contact angle depends on the equilibrium state between the three interfacial tensions shown in Figure 2.2.

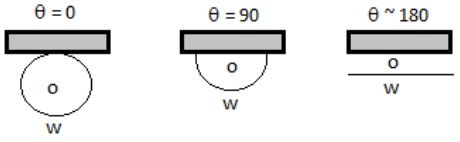

FIGURE 3.12: The contact angle is measured through the densest phase which in most cases is water. From left: water-wet case, intermediate-wet case and oil-wet case. Figure is free from Ursin and Zolotukhin (2000).

As shown by the line of action in Figure 3.13 the only preparation needed is mixing of the fluids as described in Section 3.2.

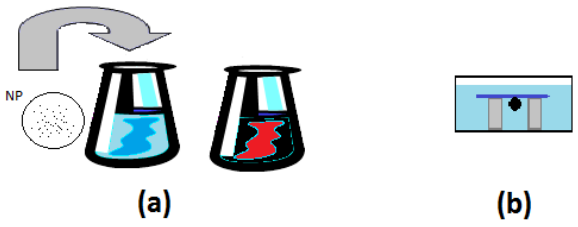

FIGURE 3.13: Schematic drawing of the line of action for the laboratory work to determine the contact angle, θ. (a) Preparation of fluids. (b) The glass box with an heavy oil droplet placed under a glass plate suspended in the water phase. The glass box is used in the Imaging method.

The setup of the Imaging Method is shown in Figure 3.14. The glass box with a smooth and clean glass plate was filled with di water or hydrophilic nanofluid. A syringe with a hooked needle was filled with heavy oil and was used to place a droplet under the glass plate as shown in Figure 3.13 (b). The glass box was then put in front of the camera. To allow for the system to reach equilibrium the oil droplet, water phase and glass plate was left to rest for at least 30 min before recordings were made. Last, the camera, computer and software "Adhesion theta" were used to take pictures of the droplet and to calculate the average of the contact angle measurements. 60 frames of 60 seconds were chosen. The results are shown in Section 5.4.

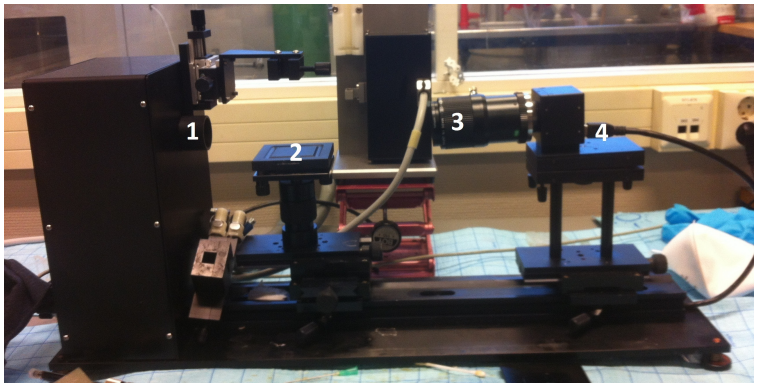

FIGURE 3.14: Set-up of the camera used for measurement of the contact angle between water, oil and a glass plate. Index 1 shows the back light, index 2 the placement of the glass box, index 3 is the camera and lens to sharpen the picture while index 4 is the cable connected to the computer.

3.5 Interfacial Tension Determination

The interfacial tension was measured using the spinning drop method. The line of action for the experiment is shown in Figure 3.15. The only preparation needed prior to the spinning drop measurement is to prepare the fluids described in Section 3.2.

3.5.1 Spinning Droplet

The spinning drop method measured the interfacial tension at 60° C. The apparatus is based on the following equation for calculation of the interfacial tension,

FIGURE 3.15: Schematic drawing of the line of action of the laboratory work that was done for measurement of the interfacial tension. (a) Preparation of fluids. (b) The Spinning drop method.

σ, (Hendranibgrat et al. 2013):

$$\sigma = \frac{\Delta\rho\Omega^2 D_{app}^3}{8n^3 J_D(\frac{L}{D})} \tag{3.9}$$

where $\Delta\rho$ is the difference in density, Ω is the rotating speed, D_{app} is the measured diameter of the drop, n is the refractive index, J_D is the correction factor and $\frac{L}{D}$ is the relation between the length of the droplet and the true diameter of the droplet which is $D = \frac{D_{app}}{n}$. Figure 3.16 shows how some of these variables are related to the spinning drop method.

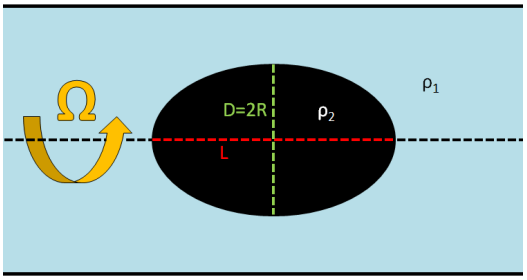

FIGURE 3.16: Sketch of the spinning droplet inside the tube filled with an aqueous phase (di water or nanofluid). Ω is the spinning rotation, L is the length and D is the diameter of the droplet. Sketch free after Hendranibgrat et al. (2013).

The input needed to be able to calculate the interfacial tension was the density of heavy oil and the water phase, and the refractive index for the aqueous phase. The density for heavy oil and the surround fluid is measured using a picknometer as described in Section 3.2.3. The results for the density of the di water and nanofluids are shown in Figure 5.1. The values of the refractive index in Table 3.1 is based on a paper by Hendranibgrat et al. (2013). They measured the refractive index of di water, 3 wt% brine and brine with nanoparticles. The results showed

a small increase of the refractive index when nanoparticles where added. For Table 3.1 it is assumed that adding nanoparticles in di water will have the same increase for the refractive index as the nanoparticle addition in brine had.

TABLE 3.1: Refractive index for Aqueous Phase based on measurements done by Hendranibgrat et al. (2013).

Fluid	Average n
Di water	1.33100
Nanofluid 0.01 wt%	1.33088
Nanofluid 0.1 wt%	1.33122
Nanofluid 0.5 wt%	1.33266

To start the spinning method first the tube was filled with a nanofluid or di water and a small droplet of heavy oil was placed inside the tube with the use of a syringe with a straight needle. The tube was placed in the apparatus and the rotation of the tube was turned on. The rotation was kept within the range of 6000 - 6200 rpm. It took about 3-4 hours until the droplet reach a stable measurement of the interfacial tension. Interfacial tension was recorded as a function of time. These results are shown in Appendix F. When the value of interfacial tension was stabilized the system had reached equilibrium.

4 Optimization of the Amott Method

Initially the Amott method was considered for investigation of the wettability of the artificial cores. Therefore both drainage and imbibition testing was performed in the optimization process. Before any experiments can be done with the use of Amott cells, two important issues has to be solved:

- The viscosity of the heavy oil: The aim was to find the correct weight percentage to mix of bitumen and dodecane to obtain a preferred viscosity of 100 cp and 200 cp at room temperature. It is also necessary to measure the viscosity at 60°C as this is the temperature the experiment is performed in.
- The diameter of the glass beads to be used in the core holder: Both spontaneous imbibition test and drainage test should result in a substantial final volume of either water or oil out of the core. The tests were done with Amott cells in an oven at 60°C for at least one week.

The results and the conclusion of the findings from the initial trials are presented in this chapter. The fluid properties of heavy oil used in the main experimental part is also given here.

4.1 Viscosity Measurement of Heavy Oil

Four viscosity measurements were done on heavy oil mixtures with different wt% of dodecane and Athabasca bitumen. To obtain the target viscosities of 100 cp and 200 cp some trial-and-error mixing and measurements was done. The viscosity

was measured with a rotating viscometer. The setup and procedure is explained in Section 3.2.4.2. The final results are shown in the Table 4.1. The viscosity at 60 °C were only measured for the mixtures that had any of the two targeted viscosities.

TABLE 4.1: Overview of the viscosity measurements on heavy oil of different wt% of dodecane and Athabasca bitumen. The aim was to obtain a heavy oil in the range of 100 - 200 cp at room temperature (22.5 °C).

Dodecane wt%	Bitumen wt%	Viscosity at room temperature	Viscosity at 60°C
22.5	77.5	580 cp	-
30	70	198 cp	29.7 cp
34	66	110 cp	19.5 cp
35.6	64.4	76 cp	-

The mixtures of 30 wt% and 34 wt% dodecane gave the targeted viscosities. The heavy oil of 30 wt% dodecane gave an viscosity of 198 cp at room temperature and 29.7 cp at 60°C. The heavy oil mixture of 34 wt% dodecane gave an viscosity of 110 cp at room temperature and 19.5 cp at 60°C. The density was only measured for the heavy oil with 30 wt% dodecane as this was the heavy oil used in the main experimental part of the thesis. The density was measured using a picknometer (see Section 3.2.3 for procedure), and the density was 0.895 g/cc. The results from the measurement can be found in Table C.5 in Appendix C.

The most interesting with heavy oil with respect to light crude oil is not the viscosity, but the difference in chemical composition as mentioned in Section 2.4.2. One key aspect is how the chemical composition may cause heavy oil and light crude oil to differ in wetting abilities when in contact with water.

4.2 Trials with Different Dimensions of Glass Beads

The diameter of the glass beads used to make the artificial cores is important due to the interaction of capillary forces and gravity forces which is where the main challenge lie. The diameter of the glass beads will affect the pore throat of the core and therefore also the capillary forces. The pore throat and pore space between the glass beads depend on the size, sorting and packing of the glass beads. The

smaller pores of the core, the stronger the capillary forces hold the oil inside the pores. However, if the pores are to large then the oil will quickly leave the core in favor of water due to gravity forces and the density difference between heavy oil and di water. In other words, the pore space and pore throats of the artificial core need to be large enough for the oil and water to spontaneously imbibe, but small enough so that the drainage process is not only due to gravity.

The glass beads that were tried out are: 300-400 μm, 425-600 μm, 1 mm and 2 mm. Table 4.1 is an overview of the trials and the results. Pictures of the end result of all ten trials can be found in Appendix B. The main points of the trials are summed up in the following sections.

All trials where put in an oven at 60°C for at least one week. The heavy oil of 200 cp at room temperature was used in trial 1 to 9. For trial 10 the heavy oil mixture of 100 cp at room temperature was used. This was to check if the smaller glass beads could be used with heavy oil with lower viscosity. The result was negative. In the imbibition tests (IMB) the artificial cores were fully saturated with heavy oil and surrounded by distilled water in the Amott cell. In the drainage tests (DRAIN) the artificial cores were fully saturated with distilled water, and they were surrounded by the chosen heavy oil mixture in the Amott cell.

TABLE 4.2: Overview of the examination trials done with Amott cells. IMB: spontaneous imbibition where the core is saturated with oil and surrounded by di water. DRAIN: drainage where the core is saturated with di water and surrounded by heavy oil. The Amott cells where left in the oven for at least one week at a temperature of 60 °C.

Trial	Dodecane wt%	Bitumen wt%	Diameter of glass beads	Filter type	Imb or Drain	V_s mL
1	30	70	300–400 μm	Plastic	IMB	0
2	30	70	1 mm	Small steal	IMB	7.7
3	30	70	1 mm	Large steal	IMB	8.1
4	30	70	2 mm	None	IMB	5.4
5	30	70	2 mm	None	DRAIN	11.9
6	30	70	425–600 μm	Small steal	IMB	0
7	30	70	425–600 μm	Small steal	DRAIN	11.9
8	30	70	425–600 μm	Small steal	IMB	0
9	30	70	425–600 μm	Small steal	IMB	0
10	34	66	425–600 μm	Small steal	IMB	0.2

The imbibition test with glass beads of 300-400 μm (Trial 1) gave no oil out of the core. This glass bead size was therefore ruled out as an option.

The drainage test of 425-600 μm (trial 7) resulted in a substantial amount of drained water. The imbibition tests of with glass beads of 425-600 μm (Trial 6 to 10) produced no oil out for any of the imbibition tests. Therefore this size was also excluded as an option. Based on the observation of no oil out in any of the imbibition tests (Trial 6 - 10) and a substantial amount of water out in the drainage test (Trial 7) of the cores with glass beads of 425-600 μm it was decided to reduce the Amott method to only the spontaneous imbibition test. In the spontaneous imbibition test the wetting of the cores will be based on the rate at which the oil escapes from the core. If it escapes fast, the core is water-wet. And the slower time it takes, the more the wettability moves towards neutral or oil-wet. The test is based on the tenancy of a rock to imbibe the wetting phase spontaneously (Denekas et al. 1959).

Not much difference for the 1 mm and 2 mm glass beads were observed. Although some filter issues with air blocking the filter has been observed. The trials with 2 mm glass beads (trial 4 and 5) were performed to investigate the end effect of the filters. The 2 mm glass beads were ruled out as an option because of the observed gravity issues. When the core was lifted out of heavy oil or di water the fluid would quickly leave the core.

4.3 Further Experimental Work

The final decision for the further experimental work based on the examination trials was as follows:

- The glass beads with a diameter of 1 mm and the heavy oil with a viscosity of 200 cp at room temperature were chosen for further experimental work.
- Due to the limitations observed in the initial trials (Trials 5 and 7), the planned Amott method will be reduced to an imbibition test which is one of the steps in the Amott method.

5 Experimental Result and Evaluation

This chapter is a summary of the results and main findings from the experimental work. An evaluation of the results from the measurements and of the experimental methods is given also given. First, the results of the nanofluid properties and core properties are given. Second, the results of the spontaneous imbibition method are shown. Then short review of all results and the preparatory conditions prior the use of the Amott cell is given. Preparatory conditions are the work before the main part of the experiment. Last, the results of the contact angle and interfacial tension measurements are shown. Some observations and evaluation of methods are given.

5.1 Properties of Nanofluids

The fluid properties density and viscosity was measured for the nanofluids and di water. Picnometer was used to measure density and the capillary viscometer was used to measure viscosity. The experimental procedure is explained in Section 3.2.3 and Section 3.2.4.1 respectively. The results can be found in Appenix C. Figure 5.1 show the values of the viscosities and densities as a function of the nanoparticles added to the di water. The fluid properties of the nanofluids do not differ much from the properties of di water. The properties of di water were measured as a reference for how accurate the chosen methods were. Only the propertied of the nanofluid with 0.5 wt% nanoparticles differs noticeably from the properties of di water.

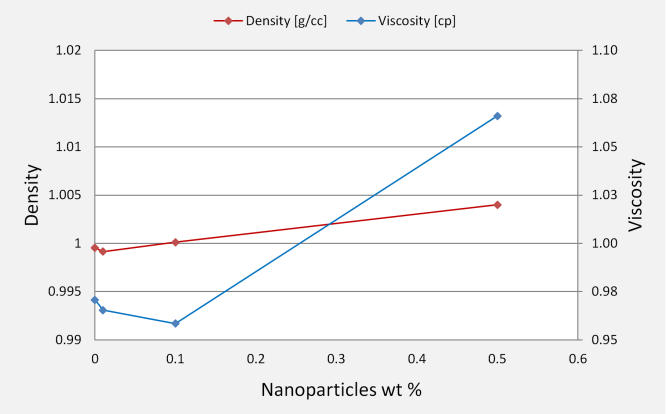

FIGURE 5.1: Viscosity and density of water and nanofluids as a function of weight percentage (wt%) of hydrophilic nanoparticles.

5.2 Measurements on Cores

The rock properties porosity and permeability was measured for the artificial cores. The porosity was measured using the helium porosimeter, and the setup and procedure is shown in Section 3.3.1. The porosity was measured on all the prepared artificial cores while permeability was only measured on the two cores made of none surface treated glass beads. The permeability was measured using a constant head permeameter with water as the flowing fluid. The setup and procedure is shown in Section 3.3.2. It was first tried with air as the flowing fluid, but the flow did not become laminar as the core has a high permeability. The permeability was not measured on the cores with surface treated glass beads as the flowing water through the core might wash away the nanoparticles attached to the surface area of the beads.

5.2.1 Porosity

The porosity was measured on every artificial core prepared, even the cores made of glass beads that had been surface treated with nanoparticles. The measurements and results for all cores can be found in Appendix D. In Table 5.1 an average is taken of the porosity value of the same type of cores. The meaning of the same type of cores is cores prepared of glass beads with same surface coating, e.g. none surface treated beads, beads soaked in 0.01 wt% hydrophilic nanofluid etc.

TABLE 5.1: Results from porosity measurements. The porosity value is an average of the cores. Measurement on each core can be found in Appendix C.

Nanoparticle	None	Hydrophilic			Hydrophobic		
Concentration [wt%]	0	0.01	0.1	0.5	0.01	0.1	0.5
Porosity [%]	34.7	35.8	35.7	36.4	34.2	36.1	37.4

Porosity is not affected by the size of the grains, but their sorting, packing and shape. The glass beads used have a spherical shape, and they used are uniform in size with a diameter of 1 mm. Due to the uniform sorting and shape of the glass beads, the main factors affecting the porosity measurements is be the arrangement of the glass beads in the core holder (the packing) and the human errors. Human errors include that the volumes are not read correctly of the porosimeter.

According Torsæter and Abtahi (2003) the maximum theoretical porosity of uniform spherical grains is 48 %, and it is achieved by perfect cubic packing. Rhombohedral packing however gives a porosity of 26 %. The results for the porosity measurement of the artificial cores shown in Table 5.1 are well within these theoretical values.

5.2.2 Permeability

The permeability was measured on two cores prepared of none surface treated glass beads. Core A gave a permeability of 10.19 D. Core B gave a permeability of 11.23 D. The measurement results are shown in Figures C.2 and C.3 in Appendix C. The permeability values are high, but they are within the limits of the expected values as the porosity is as high as 35 %. As mentioned in the result section on the porosity measurements, the cores are prepared of uniform spherical glass beads. Permeability is a function of the size, sorting, shape and packing of the glass beads. Due to the uniform shape and size of the glass beads, these factors (including sorting) do not influence the permeability difference of the cores. The only parameter influencing permeability is therefore the packing.

In the experiment the constant flow rate and the pressure drop over the core was noted. The method for measuring permeability was very sensitive in terms of stability of the flow rate, laminar/turbulent flow and the height of the fluid outlet:

- The pump used did not give a constant flow rate. The rate was therefore checked for all the measurements.

- For higher flow rates (above 5 mL/min) the flow became turbulent due to the high permeability of the cores. The turbulent flow was observed by the lack of stabilizing in the pressure drop over the core. As Darcy's law (Equation 2.2) is used for calculating the permeability the flow needs to be in the laminar flow regime. Recall that this is one of the limitations in Darcy's law.
- It was also observed a response in the measured pressure drop when the fluid outlet was shifted up and down. The pressure drop over the core was very low, and is therefore very sensitive. Based on this observation there are reasons to believe that there are flaws in some of the measurements as the fluid rate was still constant when the pressure drop effect was observed.

It is difficult to eliminate any of the limitations and errors mentioned above. The solution to the low pressure drop effect would be to increase the rate. However since the flow then becomes turbulent, this solution is dismissed. One solution would be to choose another method. However, the other method available, air permeability, could not be used either due to turbulent flow. The permeability values found are agreed upon and as they are not critical to the rest of the experimental work performed the unsure values are accepted.

5.3 The Spontaneous Imbibition Test

The spontaneous imbibition test is a qualitative method. The wettability determined in this experiment is relative, and only an estimate of alternated wettability can be determined. Therefore the results from the hydrophilic and hydrophobic experiments have to be compared with the initial experiments which represent the reference case, e.g. initial wettability. If the oil escapes faster from the core, the core is considered to be more water-wet. If the rate of oil out is slower, the wettability is considered to be changed to less water-wet or more oil-wet. Also some difference in the total oil produced from the different cases can be compared.

The preparation, setup and procedure of the spontaneous imbibition test can be found in Section 3.4.2. The measurement data, pictures of the Amott cells at the end of each measurement, and the porosity measurement of all cores can be found in Appendix D. A comparison of the hydrophilic and hydrophobic cases with

the reference case is given. Prior to the comparison the measurement results are given and the measurements with incorrect preparatory conditions are eliminated. Preparatory conditions are based on the experimental work done before the main part of the experiment such as fluid preparation, core preparation, how long the core is saturated with heavy oil, and to which temperature the equipment is heated to prior start. Correct preparatory conditions are mixing of the correct fluid weights (applies for heavy oil and nanofluids), core preparation (influence the packing of the grains and the pore structure), the core should be left saturated in heavy oil for one day, and last, the di water, saturated cores and Amott cells should be heated to 60 ^{o}C prior start of the imbibition test. Preparation that deviates from the mentioned conditions above is referred to as incorrect preparatory conditions. Last, an evaluation of the experiment is given.

5.3.1 Initial Rates

Four experiments with artificial cores made of none surface treated glass beads were done. The glass beads are assumed to be water-wet, and they have the same wettability as no surface treatment with nanofluids was done. The spontaneous oil production for the four cores are shown in Figure 5.2. These curves represent the reference case of initial wettability. Core A and B was performed together, the same was core C and D. The experiments shown in Figure 5.2 were all performed with the correct preparatory conditions. In the experiments of core A and B there was a problem with heavy oil droplets that got stuck at the inlet of the measuring tube. The droplets got stuck at the narrowing of the Amott cell as the cell has the shape of a bottleneck. The problem was solved by shaking the cell. Therefore a delay in the recorded volumes is expected. However, all four curves are considered to be representative for the reference case. The curves do not coincide well. However, they have the same shape, and the start times for imbibition of core A and B are in agreement with the start time of core D. The start time of imbibition is when the heavy oil starts to leave the core and float up into the measuring tube of the Amott cell due to the density difference with di water.

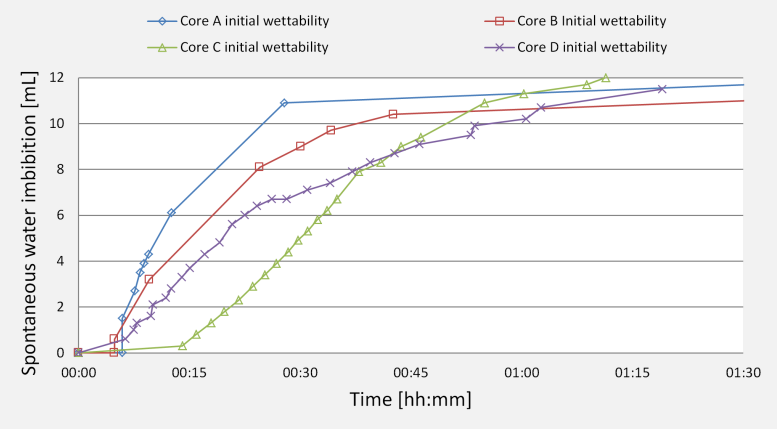

FIGURE 5.2: The rates for the reference case with initial wettability. Artificial cores with none treated glass beads were used.

5.3.2 Hydrophilic Rates

Three cases of hydrophilic experiments where performed. The three cases were artificial cores made of glass beads soaked in 0.01 wt%, 0.1wt% and 0.5 wt% hydrophilic nanofluids.

0.01 wt%

Two experiments were performed with cores made of glass beads treated with 0.01 wt% hydrophilic nanofluid. The results are shown in Figure 5.3. The cores were both saturated in heavy oil for one day, but for the experiment with core A the di water was heated above 60 degrees C. This resulted in the higher rate of water imbibition, and the curve has a steeper slope. The experiment is rejected for the comparison as the preparatory conditions are not correct. Core B is therefore the only curve representing the hydrophilic 0.01 wt% imbibition case in Section 5.3.4.

0.1 wt%

Three experiments with cores made of glass beads treated with 0.1 wt% hydrophilic nanofluid. The results are shown in Figure 5.4. Core A and B were performed together and the preparatory condition were not done correctly. The cores were put into the Amott cell the same day they were saturated, i.e. the cores were not saturated in heavy oil for one day, but for approximately 3 hours. This is discussed in Section 5.3.5. Also, for the experiment with core A, the volume of oil

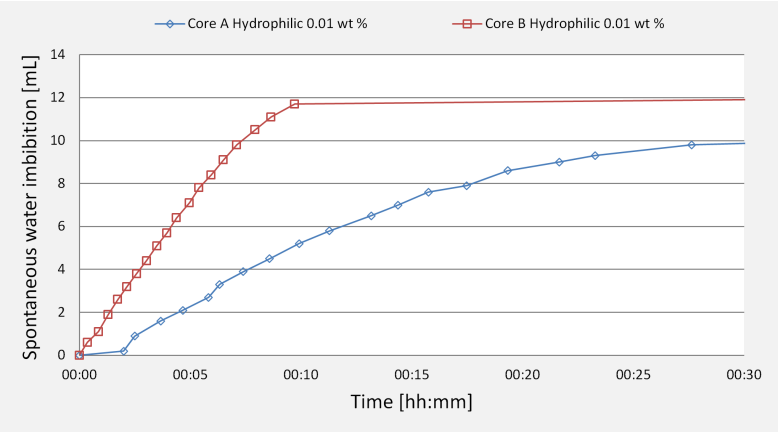

FIGURE 5.3: The rates from the experiments with 0.01 wt% hydrophilic artificial cores.

went out of the 15 mL scale as too much air was trapped in the Amott cell. The large amount of air in the Amott cell was caused by the lack of after filling the Amott cell with enough water before closing the cell with the end piece.

Due to the failure in the preparatory conditions of core A and B another core was prepared. Core C was prepared with the correct steps except for that the heavy oil was re-used after the hydrophobic measurements. This resulted in a gentler sloped curve than for core A and B. The problem with re-using heavy oil after the hydrophobic measurements is explained in Section 5.3.5. The rates for core C are therefore dismissed for comparison, and the rates of core A and B are used in Figure 5.8.

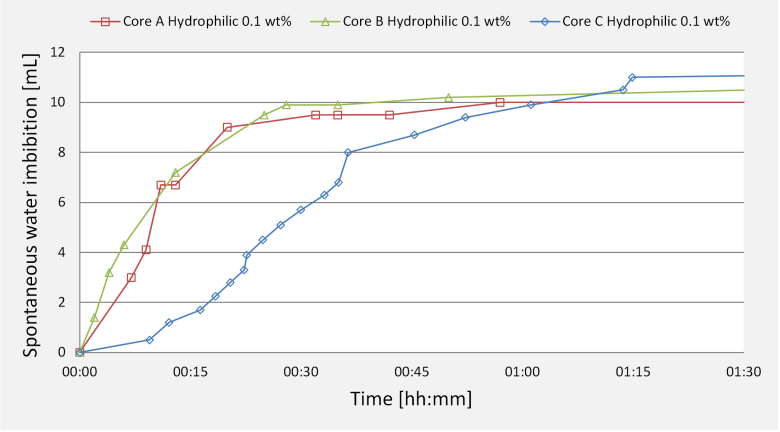

FIGURE 5.4: The rates from the experiments with 0.1 wt% hydrophilic artificial cores.

0.5 wt%

Four experiments were performed with artificial cores made of glass beads treated with 0.5 wt% hydrophilic nanofluid. The results are shown in Figure 5.5. It is the same problem as observed for the 0.1 wt% hydrophilic core C as these cores where prepared together. This resulted in a gentler sloped curve than for core A and B. The problem with re-using heavy oil after hydrophobic measurements is explained in Section 5.3.5. The rates for core C and D are therefore dismissed for comparison, and core A and B are used in Figure 5.8.

In the first two experiments (core A and B) the production of oil was higher than the volume of the scale at the Amott cell. The cells used had a scale of 10 mL. Also, the preparation was not the same as for the reference case. The cores were not saturated in oil for one day, but for approximately 3 hours. Also for sample A, the O-ring was too small for the end piece which led to leakage of air into the Amott cell.

Based on the problems encountered with core A and B, the two last experiments (Core C and D) was prepared with the correct preparatory conditions except for that the heavy oil was re-used after the hydrophobic measurements.

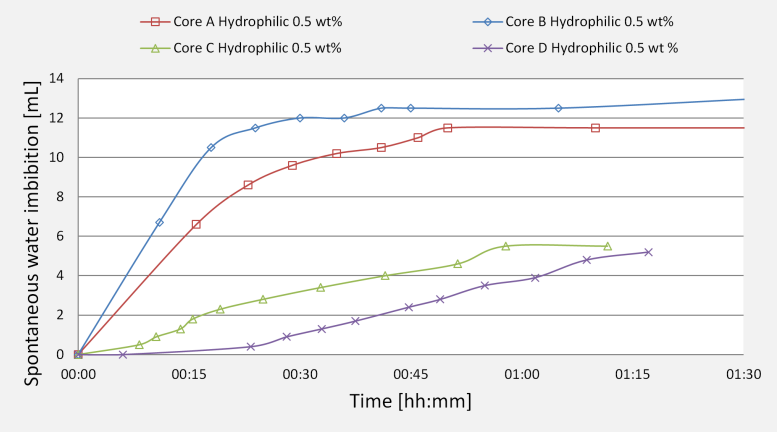

FIGURE 5.5: The rates from the experiments with 0.5 wt% hydrophilic artificial cores.

5.3.3 Hydrophobic Rates

Three cases of hydrophobic experiments where performed. The three cases were artificial cores made of glass beads soaked in 0.01 wt%, 0.1wt% and 0.5 wt% hydrophobic nanofluids.

0.01 wt%

Two experiments where done with artificial cores of glass beads soaked in 0.01 wt% hydrophobic nanofluid. The rates of core A and B are shown in Figure 5.6, and the rate of the two cores coincide well. Prior to the experiment the preparations were executed correctly, and the cores were put into the Amott cells almost simultaneously. The curves of both core A and B is used in the comparison of hydrophobic cases to the reference case in Figure 5.9.

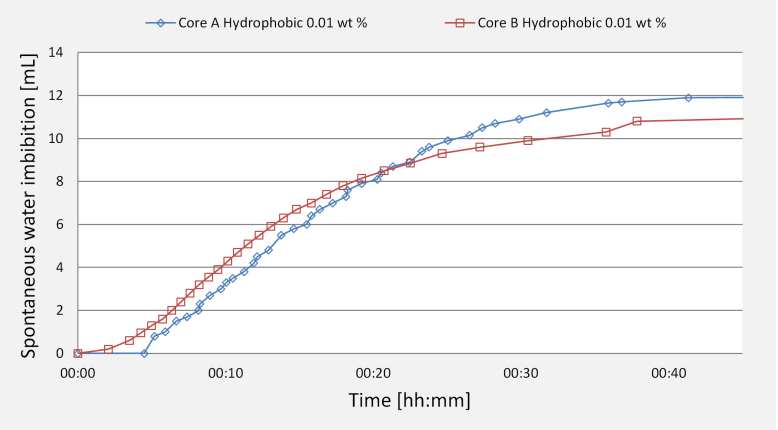

FIGURE 5.6: The rates from the experiments with 0.01 wt% hydrophobic artificial cores.

0.1 wt%

Five experiments where done with artificial cores of glass beads soaked in 0.1 wt% hydrophobic nanofluid. The results are shown in Figure 5.7. Core A and B was performed together. Core A has problems with heavy oil blockage of the measuring tube of the Amott cell. The oil did not loosen by shaking the Amott cell; hence the measurement of core A was aborted. Core C was done to verity the rates of core B, but as the core were left saturated for two days in heavy oil before the imbibition test no oil came out. The experiments with core D and E were done together and the correct preparation was executed. The rate curves of B, D and E do not coincide or have the same time until the start of imbibition, but they have a similar same slope. All three curves are chosen to represent the hydrophobic 0.1 wt% case in the comparison of the hydrophobic cases with the reference case in Figure 5.9.

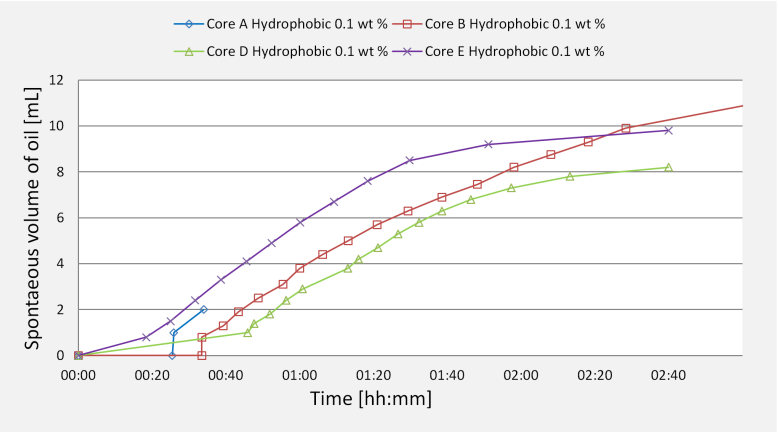

FIGURE 5.7: The rates from the experiments with 0.1 wt% hydrophobic artificial cores.

0.5 wt%

Three experiments where prepared with cores made of glass beads which had been submerged in 0.5 wt% hydrophobic nanofluid. First core A and B where prepared together, and no oil came out. The preparatory conditions were done correctly, but to be sure of the results another core was prepared. Core C did not give any oil production either. In other words, no water was spontaneously imbibed in the 0.5wt% hydrophobic case.

5.3.4 Comparison of rates and end volumes

The rate and end volume of a spontaneous imbibition depends on wettability, viscosity, interfacial tension, pore structure and initial saturation of the core (Anderson 1987a). As the viscosity of the fluids, pore structure and initial saturation ($S_w = 0$ and $S_0 = 1$) are kept constant by making sure the preparation prior the imbibition testing are correctly executed. This means that for all tests the two variables causing a change in either the end volume or the rate are wettability and interfacial tension.

Initial and Hydrophilic Rates

The rates of the reference case and the hydrophilic cases are compared in Figure 5.8. As mentioned before, the hydrophilic 0.5 and 0.1 cases where not saturated in heavy oil for one day, but only for approximately 3 hours. Therefore the

rates are not directly comparable to the hydrophilic 0.01 case and the reference case as the measurements do not have the same preparatory conditions. Ideally more imbibition testing should be done to obtain the same preparatory conditions, but it was not possible within the scope of this thesis.

The rates obtained are compared in Figure 5.8. The curves do not show a clear distinct between the different cases. But the curves of the cases with glass beads treated with hydrophilic nanofluids generally lies higher than the curves of the reference case. However, the expected increase in rate of higher concentrations of nanoparticles cannot be seen. The only conclusion drawn from Figure 5.8 is that the hydrophilic imbibition curves indicate an increase of rate (has a steeper slope) compared to the reference case. For the case of hydrophilic 0.5 and 0.1 the difference to the reference case can be a change in wettability, but it can also be due to the difference in preparatory conditions. For the hydrophilic 0.01 case, only one curve was obtained. Several curves should be produced before any conclusions are drawn.

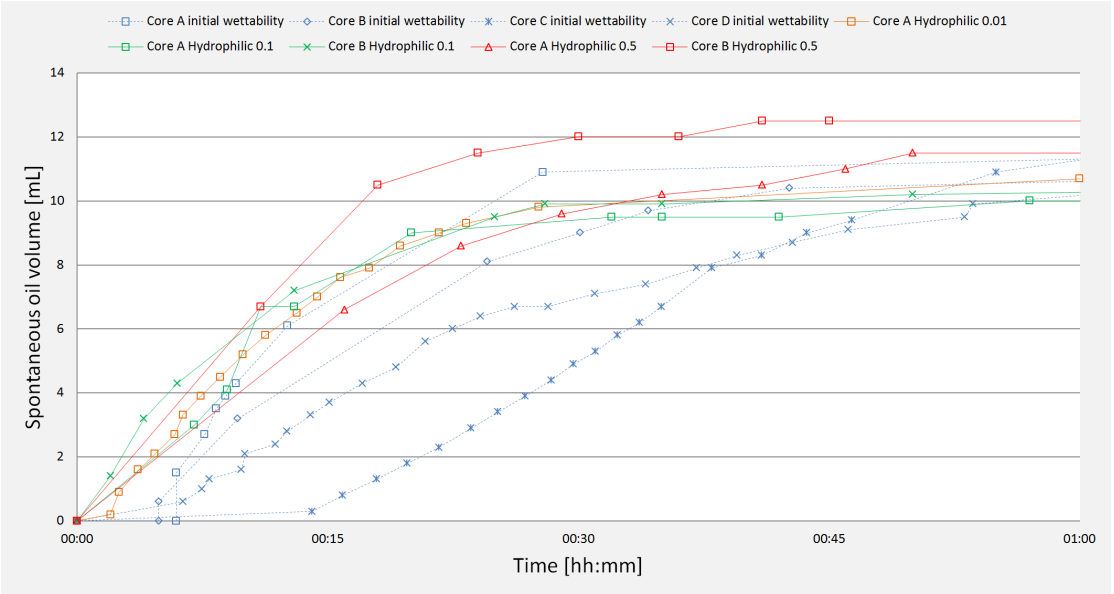

FIGURE 5.8: Comparison of the hydrophilic imbibition cases with the reference case of initial wettability.

Initial and Hydrophobic Rates

The rates from the reference case and the hydrophobic cases are compared in Figure 5.8. The hydrophilic cases and the reference case have the same preparatory conditions so they can be directly compared. The hydrophobic 0.01 case do not

show any difference in rate from the reference case. In the hydrophobic 0.1 and 0.5 case a clear change of rate compared to the reference case is be observed. For 0.5 no rate at all as hardly any oil at all came out. For 0.1 as the slope of the curve is much gentler. Also, the time until start of imbibition is longer. The conclusion based on Figure 5.8 is that settlement of hydrophobic nanoparticles impact the wettability. Also, the decrease in rate is greater for higher concentration of hydrophobic nanoparticles.

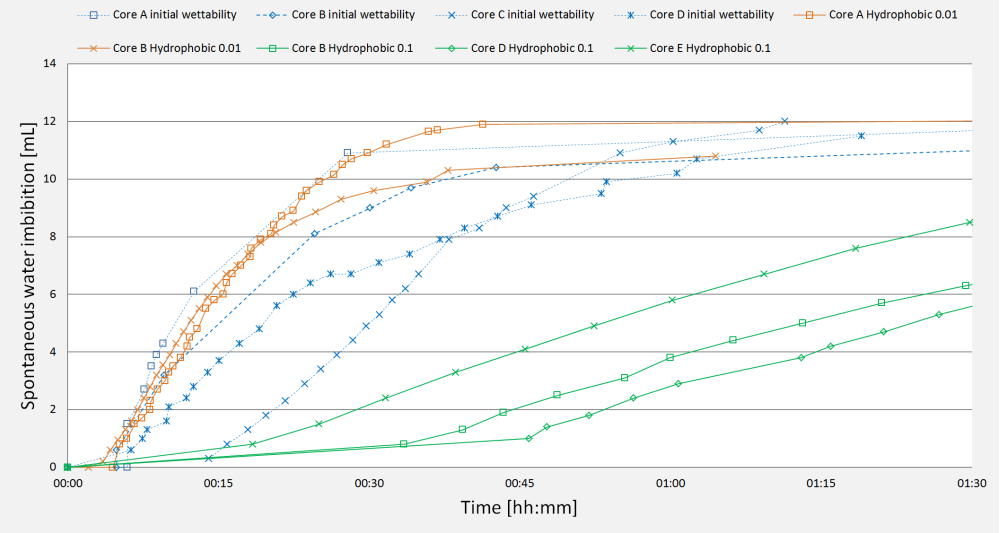

FIGURE 5.9: Comparison of the hydrophobic imbibition cases with the reference case of initial wettabilty.

End volumes

The water and heavy oil volumes in the pore space at the end of each imbibition test are shown in Figure 5.10 as bar charts. The sum of the water and oil volume shown is the total pore space of the core mentioned to the left. Unfortunately, it is hard to draw conclusions on the basis of this chart. No trend in the volumes is observed on either the hydrophilic or the hydrophobic side of the chart.

As some problems were encountered in the hydrophilic 0.1 and 0.5 wt% measurements, so neither of the end volumes for these cases are entirely correct. Also, the hydrophilic 0.01 wt% case show the same production as the reference cases (called initial wettability in Figure 5.10). A trend on the hydrophobic side is not observed either as the 0.01 wt% and 0.1 wt% hydrophobic cases also has about the same recovery as the reference case and the hydrophilic cases. An exception is the 0.5 wt% hydrophobic case which more or less produced no oil.

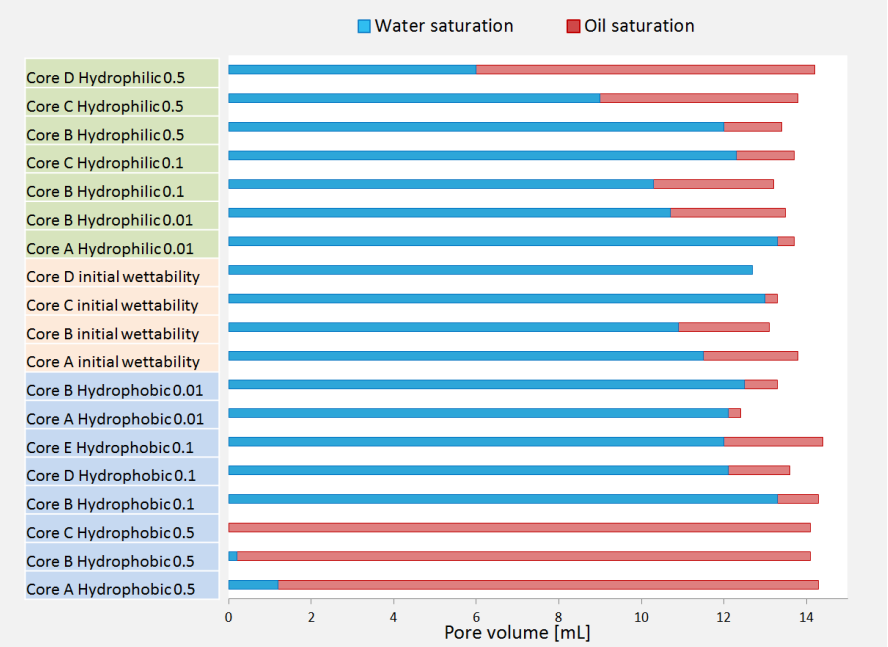

FIGURE 5.10: The bar chart represents the pore volumes of the relevant cores. The red is the oil left in the pore volume while the blue is the volume of water that was imbibed into the core.

5.3.5 Evaluation of method

Several problems were encountered during the imbibition testing and experience concerning the experiment was gained. The main challenges are summarized below, and the main learning points are given.

Encountered Problems

There were problems experienced with re-using the heavy oil in hydrophilic imbibition testing after using it in the hydrophobic tests. The indication of the problem is that the rates obtained from the experiment was much lower than for the reference case as if the hydrophilic nanoparticles have no effect the rate should be the same as the reference case. The problem may be due to the presence of hydrophobic nanoparticles in the heavy oil, and when the hydrophilic nanoparticles are present in the di water it may have led to an increase of interfacial tension as the nanoparticles will make the phases repel each other.

Next, lack of experience in the laboratory and with the experimental method led to several mistakes in the first experiments. The main error performed was in the preparation of the experiment. These were not letting the core stay saturated in

heavy oil for one day, the use of an Amott cell with a too small measuring tube and improper cleaning. Improper cleaning lead to blockage of the measuring tube of the Amott cell as it is shaped as a bottleneck. In some cases the heavy oil lost its grip by shaking the cell.

Last, based on Figure 5.10 most of the cores obtained a very high recovery rate. There might be a problem that the optimization process explained in Chapter 4 was too short. However, it had to be kept short due to the time limitation of the thesis.

Learning Points

The main learning points for the spontaneous imbibition test are important and can be used in the next wettability investigation of heavy oil. The main learning points based on Section 5.3.5 were:

- Keep the preparatory conditions stable. Experience with the method performed is important.
- Proper cleaning is important as the heavy oil is sticky and easily attaches to glass. Proper cleaning is done by first cleaning with toluene, then with methanol and last properly cleaning with soap and water. The cleaning is important for the core holders and the Amott cell.

5.4 Contact Angle

Measurement of the contact angle was done with use of the Imaging Method. The preparation, setup and procedure are shown in Section 3.4.3. The contact angle of a heavy oil droplet placed under a glass plate submerged in an aqueous phase is measured. The aqueous phases were di water and three nanofluids with 0.01 wt%, 0.1 wt% and 0.5wt% of hydrophilic nanoparticles.

5.4.1 Results

The results from the measurements are shown in Figure 5.11 where the contact angle is plotted against the record time. 60 measurements were made for the 60

frames recorded. There was one minute between each picture taken. The contact angle is given through the denser water phase. A decrease in contact angle is an indication of a more water-wet condition.

The values in Table 5.2 are an average over the 60 frames for the contact angle. A comparison of the measurements and the average is given in Appendix E. The average value is considered to be good for the nanofluid cases, but not for the di water case. The averaged line (purple) is below most of the measurements in Figure E.1. Therefore, by removing the deviating results a better average may be found. By doing so, a contact angle average of 28.05^o was found for the di water.

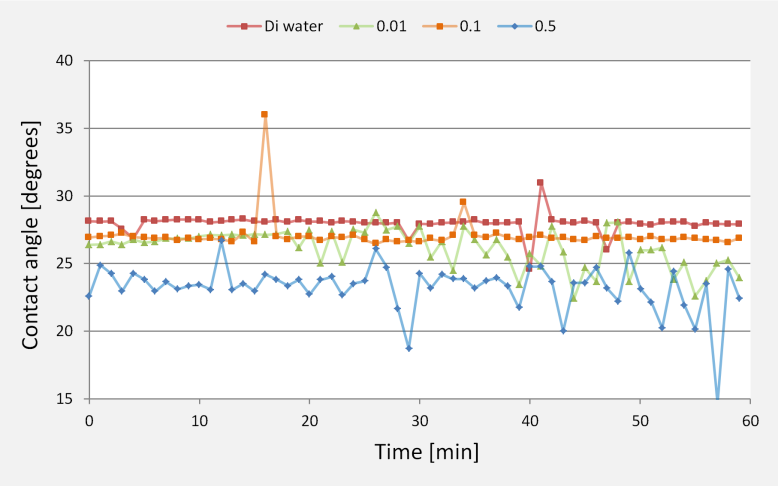

FIGURE 5.11: Contact angle results from the imaging method for all cases as a function of the recorded time is shown in the graph.

TABLE 5.2: Calculated averages of the frames recorded. All nanoparticles used were hydrophilic.

Aqueous phase	Di water	0.01 wt %	0.1 wt %	0.5 wt %
Mean Contact angle [degrees]	28	26.19	26.68	23.38
Standard deviation [degrees]	0.70	1.43	1.20	1.68

5.4.2 Observations

Figure 5.12 show vertically flipped images of the frames recorded during the measurements, one for each water phase. From the figure it is clear that the higher nanoparticle concentration, the less transparent the water phase is and the difficulty of focusing the camera on the droplet and glass edge increases. As the concentration of nanoparticles increased in the water phase, the same did the difficulty of placing the heavy oil droplet under the glass plate and the difficulty of

focusing the camera on the droplet. The pink line and the red line are the estimations of drop shape and contact angle given by the software "Attetion Theta". Less transparency of the fluid or impurities in the picture makes it difficult for the software to do the estimations. This may be one of the causes of the fluctuating results shown in the contact angle of 0.5 hydrophilic nanofluid.

Also, it was observed that the software had difficulties estimating low values of the contact angle through the water phase.

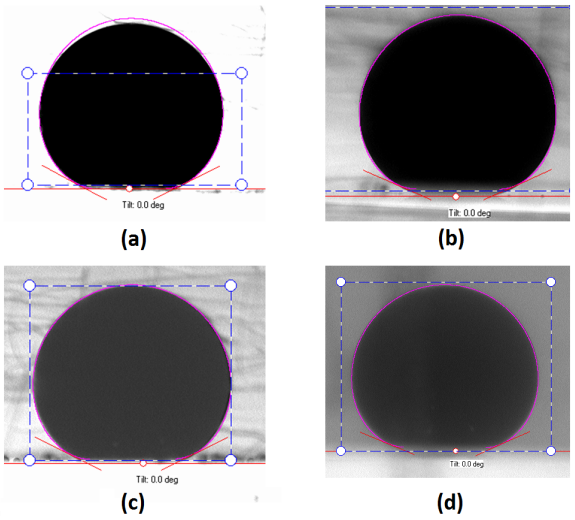

FIGURE 5.12: Vertically flipped frames recorded during the measurements. The pictures show the heavy oil droplet placed under a glass plate submerged in an aqueous phase. The aqueous phases are: (a) di water and nanofluids with (b) 0.01 wt% (c) 0.1 wt% and (d) 0.5 wt% of hydrophilic nanoparticles.

Equilibrium Issues

The main challenge encountered measuring the contact angle measurement was the time for the system to reach equilibrium. Equilibrium of the system is reached when the contact angle is constant through time. The system was left at room temperature for 30 minutes to let the fluid system approach the equilibrium state. For the results shown in Figure 5.11 the results of the contact angle for 0.1 and di water have the best repeatability while the results for 0.01 and 0.5 fluctuates. The low repeatability of 0.01 and 0.5 is caused by the lack of system equilibrium which is needed for the contact angle to reach a stable value prior the start of the imaging method. The fluctuations of 0.5 can also be caused by the poor picture quality as discussed above.

5.5 Interfacial Tension

The interfacial tension between oil and four aqueous phases was measured. The aqueous phases where di water, and 0.01 wt%, 0.1 wt% and 0.5 wt% hydrophilic nanofluids. The interfacial tension was measured with the use of the spinning method. The preparation, setup and procedure are explained in Section 3.5.

5.5.1 Results

The results of the interfacial tension measurements are shown in Table 5.3. In Appendix F the interfacial tension and temperature measurements are plotted as a function of record time. Also the final interfacial tension value is added. The interfacial tension values in Table 5.3 are an average of the interfacial tension measurements after stabilization. As a rule of thumb, the measurement was considered stable when the measurement had been constant for at least 15 min. The nanofluids gave lower interfacial tension measurements than the case of di water did. The discussion is given in Chapter 6. Figure 5.13 show pictures of the spinning heavy oil droplets.

TABLE 5.3: Calculated values from software. All nanoparticles used were hydrophilic.

Fluid	Di water	0.01	0.1	0.5
$IFT_{average}$	5.54	5.213	5.439	5.27
$T_{average}$	59.99	59.87	60	60
From [s]	10998	10996	13771	13851
To [s]	12480	12898	15803	14815
Average over	25 min	32 min	34 min	16 min

5.5.2 Encountered Issues

The main challenges encountered during the spinning drop method were improper cleaning and air in the spinning tube which both gave inaccurate measurements. When experience with the spinning method was gained, it was easier to discover the errors based on the behavior and shape of the droplet and shape of the interfacial tension curve.

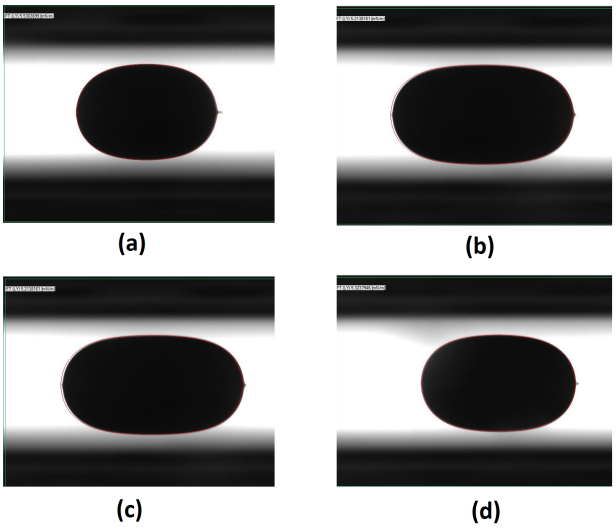

FIGURE 5.13: Screen prints of the droplet recorded by the camera. The pictures show a heavy oil droplet which was placed in a rotating tube filled with an aqueous phase. The aqueous phases are: (a) di water and nanofluids with (b) 0.01 wt% (c) 0.1 wt% and (d) 0.5 wt% of hydrophilic nanoparticles.

Improper Cleaning

Cleaning of the spinning glass tube was done with toluene and methanol. These are strong solvent so the importance of rinsing properly with di water after cleaning and proper drying was experienced.

Air Bubbles in the Spinning Tube

First, the spinning glass tube was first filled with the aqueous phase. Second, a droplet of heavy oil was placed inside the tube using a syringe. The placement of the heavy oil droplet and closing the tube without any air bubbles was the most difficult part of the experiment. Air bubbles in the tube ruins the experiment.

6 Comparison of Results

This chapter presents a comparison of the experimental results given in Chapter 5. The results will also be findings are also compared to the understanding of nanoparticle behavior and effect given by the literature presented in Chapter 2.5.

The promise of developing nanofluid into an enhanced oil recovery method is based on its ability to influence the wettability and the interfacial tension. This ability is interesting towards heavy oil reservoirs as the heavier polar components in heavy oil may attach to the pore walls and make the sandstone less water-wet. The distribution of fluid is important for the displacement process and may affect the relative permeability of the heavy oil.

The contact angle and interfacial tension are related as shown by Young's law (Equation 2.6). The contact angle, and therefore also the wettability, are dependent of the equilibrium state of the interfacial tensions shown in Figure 2.2. The interfacial tension measurements performed in the present thesis is the tension between heavy oil and the aqueous phases, σ_{wo}. The results of the interfacial tension and contact angle are plotted together in Figure 6.1. In Table 5.2 the results for the contact angle measurement are given. The results for the interfacial tension measurement are given in Table 5.3. The measurements are performed at different temperatures, and can therefore not be compared directly, but the trend of their curves can give an indication of the equilibrium state and the effect of hydrophilic nanoparticles present in the di water. The curves in Figure 6.1 have the same behavior. The curves for both the contact angle and the interfacial tension decrease when nanoparticles are present. 0.5 wt% nanofluid gave lower values than 0.1 wt% which is consistent with the hypothesis given in the Introduction. However, 0.01 wt% nanofluid gave lower values the 0.1 wt% nanofluid for contact angle and interfacial tension. This result contradicts the hypothesis given in the introduction. 0.01 wt% nanofluid gave the lowest value for interfacial tension and the second

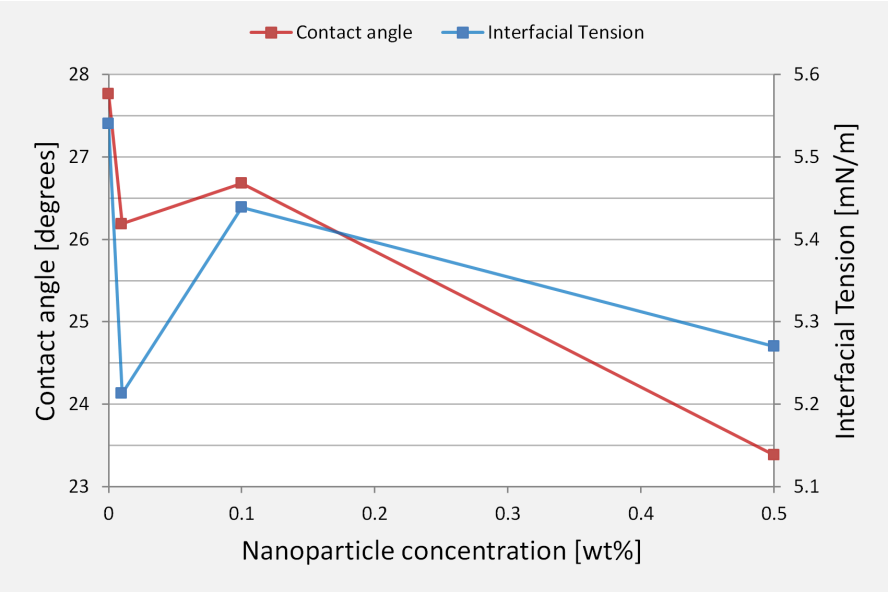

FIGURE 6.1: The measured values for interfacial tension and contact angles of a two-phase system of heavy oil and aqueous phase. All nanoparticles used were hydrophilic.

lowest value for the contact angle. The reason for the lower values of 0.01 wt% nanofluid is not clear. It is easy to jump to the conclusion of measurement errors. However, as the same trend is shown for both curves it is unlikely that the result are not caused by measurement errors as the trend has been verified by two experimental measurements. The repeatability of the results from the contact angle measurement and the interfacial tension measurement was not tested. Repeatedly measurements and comparison of the results are needed to investigate the possibility cause of measurement errors causing the effect of the low values for the case of 0.01 wt% nanofluid.

The observed drop in the curves where not observed by Hendranibgrat et al. (2013). They investigated the effect of nanoparticle concentration in nanofluids on interfacial tension and contact angle for a light crude oil and brine as the basefluid. The contact angle was measured for nanofluids with a nanoparticle concentration up to 0.1 wt%. The increasing concentration gave a decrease in the contact angle. The interfacial tension was measured for nanofluids with a nanoparticle concentration up to 0.05 wt%. The increasing concentration also gave a decrease in the interfacial tension.

The spontaneous imbibition test investigated the effect of nanoparticle absorption on the wettability. The imbibition testing with hydrophilic nanofluids had limited success as the preparatory conditions were not optimal for all cases. Together with

the hydrophobic nanofluids however, an indication by rate change was observed. However, whether the change in rate was caused by interfacial tension change or altered wettability is not clear. It is likely that the observed rates are results of both causes.

The theory in Section 2.5.4 is based on papers by several authors and a short summary of the main findings are:
The wettability conditions is changed when one of the liquids contain nanoparticles(Chaudhury 2003). Silica nanoparticles may alter the wettability of the rock matrix based on the chosen surface coating of the nanoparticles and the amount of particles absorbed on the pore wall. Nanoparticle flooding may also reduce interfacial tension by positioning itself on the interface between oil and water (Hendraningrat et al. 2012).

The findings in the literature are consistent with the observations in this thesis. In general, all experiments point in the direction of a wettability and interfacial tension alternation by silica nanoparticles, hydrophilic or hydrophobic. However, some limitations met in the experimental work make it hard to conclude on the quantitative effect induced. More experimental work is needed and future recommendation of work is given in Chapter 8.

7 | Concluding remarks

The final concluding remarks are:

- Nanofluids promise an alternation of the wettability and the interfacial tension. The expected change depends on the type of nanoparticle chosen and the concentration of nanoparticles in the nanofluid.
- The spontaneous imbibition test was imprecise and had low repeatability for most of the core types used. Either more optimization of the method is required or other methods should be considered. However, based on the water imbibition curves a change in rates for the different cases were observed which is likely to be caused by an alternation in wettability and interfacial tension.
- The contact angle and interfacial tension was altered by the presence of hydrophilic nanoparticles in the di water. Though, a deviation in the expected behavior when comparing the results was observed.
- With the imaging method it is difficult to get accurate measurements of the contact angle on strongly water-wet surfaces. Also, nanofluids with a high concentration of nanoparticles are less transparent than di water. This makes it difficult to focus on the droplet and the glass plate edge at the same time.
- Based on the experimental work performed it is concluded that nanoparticles have an effect on the interfacial tension and the wettability. It is also observed that the concentration has an impact.

8 Further Work

Based on the findings of this thesis and the challenges encountered in the experimental work some recommendations of further work are made:

- Perform the spontaneous imbibition test with new hydrophilic treated cores which have the same preparatory conditions as the reference case.
- Alternatively, continue the optimization process further. It is suspected that the production of the heavy oil of 198 cp (at room temperature) in 1 mm glass bead cores are dominated by gravity drainage, hence the similar end volume for most of the cores. The optimization may led to the possibility of performing the Amott method. The Amott method can provide a quantitative measure for the wettability which is helpful for quantifying the wettability alternation.
- The repeatability of the contact angle and interfacial tension measurements should be checked. Preferably these measurements should be performed at the same temperature. The same temperature will give the measurements the same type of conditions, and the results are more relevant for comparison.
- Nanoparticles are promised to increase the thermal ability of heat transfer fluids such as water. Investigation of the thermal properties of nanoparticles are highly relevant for heavy oil as the enhanced oil recovery techniques today are aims to lower the viscosity through introducing heat to the reservoir. It would be interesting to see how the thermal ability works together with the interfacial tension disturbance by nanoparticles as heat also reduces the interfacial tension.

Nomenclature

A	-	Area
D or d	-	Diameter
D_{app}	-	Apparent (measured) diameter
g	-	Gravity constant, 9.81 m/s^2
J_D	-	Correction factor for the spinning drop method
k	-	Permeability or konstant for the capillary viscometer
$k_{e\alpha}$	-	Effective permeability of oil, water or gas
$k_{r\alpha}$	-	Relative permeability of oil, water or gas
L	-	Length
n	-	Refractive index
p	-	Pressure
p_c	-	Capillary pressure
p_{nw}	-	Pressure in non-wetting phase
p_w	-	Pressure in wetting phase
q	-	Flow rate
r	-	Radius
r_o	-	Displacement-by-water ratio
r_w	-	Displacement-by-oil ratio
S_α	-	Saturation of oil, water or gas
S_{or}	-	Residual oil saturation
S_{wc}	-	Connate water saturation
S_{wr}	-	Irreducible water saturation
SG	-	Specific gravity
T	-	Temperature
t	-	Time
u	-	Flow velocity
V	-	Volume
V_α	-	Volume of oil, water or gas
V_b	-	Bulk volume
V_g	-	Grain volume
V_p	-	Pore volume
w	-	Weight

α	-	Referes to oil (o), water (w) or gas (g) phase
Δp	-	Pressure difference
$\Delta\rho$	-	Density difference
ϕ	-	Porosity
γ	-	Specific gravity or shear rate
λ	-	Mobility
μ	-	Dynamic or aboslute viscosity
θ	-	Contact angle
ρ	-	Density
σ	-	Surface or interfacial tension
τ	-	Shear stress
υ	-	Kinetic viscosity
Ω	-	Rotation speed
API	-	American Petroleum Institute
EOR	-	Enhanced oil recovery
IFT	-	Interfacial tension
WI	-	Wettability index
wt%	-	Weight percentage

Bibliography

Anderson, W. (1986). Wettability literature survey - part 2: Wettability measurement. *Journal of Petroleum Technology.*

Anderson, W. (1987a). Wettability literature survey - part 4: Effects of wettbility on capillary pressure. *Journal of Petroleum Technology.*

Anderson, W. (1987b). Wettability literature survey - part 5: The effects of wettbility on relative permeability. *Journal of Petroleum Technology.*

Ashrafi, M., Souraki, Y., Karimaie, H., and Torsæter, O. (2011). Experimental pvt property analyses for athabasca bitumen. *Pressented at the Canadian Unconventional Resource Conference held in Calgary, Alberta,Canada, 15-17 November 2011.* SPE 147064.

Aylward, G. and Findlay, T. (2002). *SI Chemical Data, 5th edition.* John Wiley & Sons Australia, Ltd, second edition edition. Monograph Volume 20.

Caldelas, F., Murphy, M., Huh, C., and Bryant, S. (2011). Factors governing distance of nanoparticle propagation in porous media. *Paper SPE142305 was prerpered for presenation at the SPE Production and Operations Symposium held in Oklahoma city, USA.*

Chaudhury, M. (2003). Spread the word about nanofluids. *Nature Publishing Group, www.nature.com/nature.*

Dake, L. (1978). *Fundamentals of Reservoir Engineering.* Development in Petroleum Science. Elsevier. Reprinted 2006.

Denekas, M., Mattax, C., and Davis, G. (1959). Effects of crude oil components on rock wettability. *Presented at the AIChE-SPE Joint Symposium in Kansas City, Mo. (SPE 1276-G).*

Enderby, J. and et al. (2004). Nanoscience and nanotechnologies: opportunities and uncertainties. Published by The Royal Society & The Royal Academy of Enginnering at www.nanotec.org.uk/finalReport.htm.

Evdokimov, I. N., Eliseev, N. Y., Losev, A. P., and Novikov, M. A. (2006). Emerging petroleum-oriented nanotechnologies for reservoir engineering. *The SPE Russian Oil and Gas Technical Conference and Exhibition held in Moscow, Russia.*

Glover, P. (2011). Chapter 7: Wettability. Formation Evaluation MSc Cource Notes.

Guo, H. (2011). Aes1300 properties of hydrocarbons and oilfield fluids. TU Delft lecture notes.

Hardage, B. (2009). Possible nanotechnology application in petroleum reservoirs. *The Geophysical Corner Column, AAPG Explorer.*

Hendranibgrat, L., Li, S., and Torsæter, O. (2013). A coreflood investigation of nanofluid enhanced oil recovery in low-medium permeability berea sandstone. *Prepared for the SPE Internation Symposium on Oilfield Chemistry held in The Woodlands, Texas, USA, 8-10 April.*

Hendraningrat, L., Shidong, L., Suwarno, and Torsæter, O. (2012). A glass micromodel experimental study of hydrophilic nanoparticles rentention for eor project. *SPE paper 159161 presented at the SPE Russian Oil & Gas Exploration & Production Technical Conference and Exhibition, Moscow, Russia, 16-18 of October.*

Kong, X. and Ohadi, M. M. (2010). Application of micro and nano technolgies in the oil and gas industry - an overwiew of the recent progress. *Paper SPE138241 was prepered for presentation at The Abu Dhabi International Petroleum Exhibition & Conference held in Abu Dhabi.*

Li, Y., Zhou, J., Tung, S., Schneider, E., and Xi, S. (2009). A review on development of nanofluid preoaration and characterization. *Power Technology*, 196. www.elsevier.com/locate/powtec.

Luthi, S. (2011). Aes3820 petroleum geology. TU Delft lecture notes.

Marshak, S. (2006). *Essentials of Geology.* W. W. Norton & Company, second edition edition.

Moon, T. (2010). Nanofluid technology promises large-scale performance gains from tight reservoirs. *JPT online.*

Parsegian, V. (2006). *Van der Waals Forces: A Handbook for Biologists, Chemists, Engineers, and Physicists.* Cambridge University Press.

Rosen, W. (2011). Aes1310-10 rock fluid interaction. TU Delft lecture notes.

Saidur, R., Leong, K., and Mohammad, H. (2010). A review on applications and challanges of nanofluids. *Elsevier.*

Schlumberger (2013). Oilfield glossary. www.glossary.oilfield.slb.com.

Schulte, W. (2012). Aes1340 applied reservoir engineering and simulation. TU Delft lecture notes.

Serrano, E., Rus, G., and Martinez, J. (2009). Nanotechnology for sustainable energy. *Renew Sust Energy Rev.*

Skauge, T., Hetland, S., Spildo, K., and Skauge, A. (2010). Nano-sized particles for eor. *Paper SPE129933 presented at the SPE Improved Oil Recovery Symposium held in Tulsa, Oklahoma, USA.*

Speight, J. G. (2009). *Enhanced recovery methods for heavy oil and tar sands.* Gulf Publishing Company.

Torsæter, O. and Abtahi, M. (2003). Experimental reservoir engineering laboratory workbook. Department of Petroleum Engineering and Applies Geophysics, Norwegian University of Science and Technology.

Ursin, J. R. and Zolotukhin, A. (2000). Introduction to petroleum reservoir engineering. Høyskoleforlaget, Norwegian Academic Press.

van Kruijsdijk, C. (2012). Aes1460 heavy oil. TU Delft lecture notes.

Wasan, D., Nikolov, A., and Kondiparty, K. (2011). The wetting and spreading of nanofluids on solids: Role of the structural disjoining pressure. *Current Opinion in Colloid & Interface Science, Elsevier.*

Yu, W. and Xie, H. (2011). A review on nanofluids: Preparation, stability mechanisms, and applications. *Article ID 435873, Journal of Nanomaterials.*

Zhang, T., Davidson, A., Bryant, S., and Huh, C. (2010). Nanoparticle-stabilized emulsion for applications in enhanced oil recovery. *SPE paper 129885 prepared for presentation at the SPE Improved Oil Recovery Symposium, Tulsa, Oklahoma, USA.*

Appendices

A Properties of Experimental Materials

A.1 Nanoparticles

Table A.1: Properties of the AEROSIL silica nanoparticles.

Properties	Unit	Typical Value	
Behaviour towards water		Hydrophilic	Hydrophobic
Specific Surface Ares *(BET)*	m^2/g	130 ± 25	110 ± 20
Average Primary Particle Size	nm	16	16
Tapped Density *(approximate value)*	g/L	50	50
Densified material *(suffix „V")*	g/L	120	90
Loss on Drying *(2 hours at 105 °C)*	wt%	≤ 1.5	≤ 0.5
Loss on Ignition *(2 hours at 1000 °C)*	wt%	≤ 1.0	≤ 2.0
pH		3.7 – 4.7	3.6 – 4.4
SiO_2-content	wt%	≥ 99.8	≥ 99.8
CAS-No.		112945-52-5 ex. 7631-36-3	68611-44-9

A.2 Organic and Inorganic Compounds

TABLE A.2: Property table for water (which is an inorganic compound) (Aylward and Findlay 2002).

Name	Water (oxide)
Chemical Formula	H_2O
Molecular weight	18.0
Density at 25°C [g/cm^3]	1.0
Boiling temperature at 1 atm [°C]	100
Melting temperature [°C]	0

TABLE A.3: Property table for organic compounds used in the experiments (Aylward and Findlay 2002).

Name	Dodecane	Ethanol (ethyl alcohol)
Chemical Formula	$CH_3(CH_2)_{10}CH_3$	CH_3CH_2OH
Molecular weight	170.3	46.1
Density at 25°C [g/cm^3]	0.745	0.785
Boiling temperature at 1 atm [°C]	216.3	78.3
Melting temperature [°C]	-9.6	-114.1

B | Initial Trials with Amott Cells

Trials with Amott cells where done to try out different glass beads sizes. The important factors of the trials are: oil imbibition and water imbibition, i.e. if there is any production of oil or water, and the end volume produced. Pictures of result from these trials can be found in this appendix. The trials were performed for optimization of the Amott method experiment. The way of deciding on next step is: trial-and-error.

B.1 300–400 μm

Trial 1

Trial 1 was the only imbibition test performed with glass beads with diameter in the range of 300–400 μ and with the use of a plastic filter. The Amott cell was left in the oven at 60°C for one week. No oil was observed out of the core. Suspect that the filter may be holding the oil back or that the viscosity is top high for this size of glass beads.

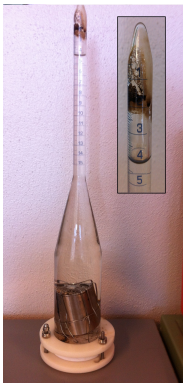

FIGURE B.1: Trial 1, IMBIBITION: artificial core made of 300-400 μ m glass beads and plastic filter. 60 °C in oven. Heavy oil mixture of 30 wt% dodecane and 70 wt% bitumen, and distilled water were used in the trial.

B.2 1 mm

Trial 2

Due to the suspicion of too small glass beads, and therefore to small pore throats, the diameter of the glass beads where increased to 1 mm. Trial 2 was also an imbibition test with the heavy oil mixture of 70 % bitumen as the saturating fluid and distilled water as surrounding fluid. The filter used was of steel with finer openings. The size of the openings was increased compared to Trial 1. First day 3.5 mL oil came out. The Amott cell was left in the oven for over one week at 60°C. Final spontaneous oil volume measured was 7.7 mL. Note after trial, still suspect that the filter openings are too small.

FIGURE B.2: Trial 2, IMBIBITION: artificial core made of 1 mm glass beads and small steel filter. 60 °C in oven. Heavy oil mixture of 30 wt% dodecane and 70 wt% bitumen, and distilled water were used in the trial.

Trial 3

Same as Trial 2, except that filter openings was increased yet again. The final spontaneous oil volume was 8.1 mL.

B.3 2 mm

2 mm glass beads were tried to have an experiment without filters for elimination of the problem. The 2 mm glass beads do not go through the holes at each end of the core holder.

Trial 4

The heavy oil mixture used was still 70 % bitumen. Oil came out fast when the

FIGURE B.3: Trial 3, IMBIBITION: artificial core made of 1 mm glass beads and larger steel filter. 60 °C in oven. Heavy oil mixture of 30 wt% dodecane and 70 wt% bitumen, and distilled water were used in the trial.

artificial core was put into the Amott cell. The oil out after 10 min was 1 mL. The core was left in the oven at 60°C for more than one week. Final spontaneous oil volume was 5.4 mL. It was observed that oil had a tenancy to cling onto the core holder. This may be due to bad cleaning after the core holders were made in the work shop. For further experiments thorough cleaning is necessary to avoid this problem.

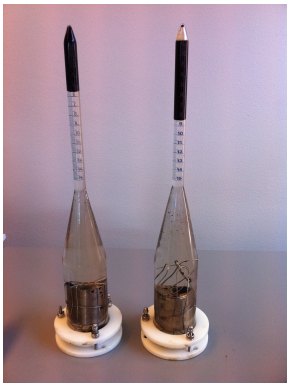

FIGURE B.4: Trial 2 to the right and trial 4 to the left, both are IMBIBITION: see Figure B.2 for details on trial 2. Trial 4: artificial core made of 2 mm glass beads and no filter. 60 °C in oven. Heavy oil mixture of 30 wt% dodecane and 70 wt% bitumen, and distilled water were used in the trial.

Trial 5

Trial 5 was the first spontaneous drainage trial. The experiment was prepared by Dr Student Shidong Li. The artificial core was fully saturated with distilled water, and a heavy oil mixture of 70 wt % was used as the surrounding fluid. The Amott cell was left in the oven at 60°C for over one week. The final spontaneous water volume was 11.4 mL.

FIGURE B.5: Trial 5, DRAINAGE: artificial core made of 2 mm glass beads. 60 °C in oven. Heavy oil mixture of 30 wt% dodecane and 70 wt% bitumen, and distilled water were used in the trial.

B.4 425–600 μm

Glass beads with diameter in the range of 425–60 μm were tried out due to the large end volume produced with the larger glass beads (1 mm and 2 mm). The finer filter of steel where used in both ends in all trials 6 to 10.

Trial 6

First trial with the use of 425–600 μm glass beads. No oil came out after one week in oven at 60°C. Suspect that air bubbles are blocking the filter.

Trial 7

Trial 7 was the only drainage trial with the use of 425–600 μm glass beads. The final spontaneous water volume after one week in oven at 60 °C was 11.9 cL.

FIGURE B.6: Trial 7, DRAINAGE: artificial core made of 425 – 600 μm glass beads and small steel filter. 60 °C in oven. Heavy oil mixture of 30 wt% dodecane and 70 wt% bitumen, and distilled water were used in the trial.

Trial 8

Same as Trial 7 except tried to block the ends with plastic to avoid air getting into core when it is lifted out of the oil and into the Amott cell with distilled water. Unsuccessful as no oil came out of the core after one week in the oven at 60 °C.

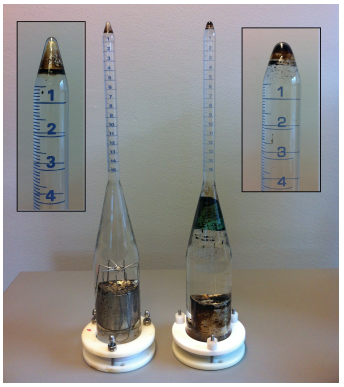

FIGURE B.7: Trial 6 and 8, IMBIBITION: artificial core made of 425 – 600 μm glass beads and small steel filter. 60 °C in oven. Heavy oil mixture of 30 wt% dodecane and 70 wt% bitumen, and distilled water were used in the trial.

Trial 9

Same test as trial 7, except that the glass tank used for saturating the cores was placed in an oven and heated for two hours at 80 °C. The glass box was not equalized with atmospheric pressure before it was put into oven. Still, no oil came out of the core after one week in the oven at 60 °C.

FIGURE B.8: Trial 9, IMBIBITION: artificial core made of 425 – 600 μm glass beads and small steel filter. 60 °C in oven. Heavy oil mixture of 30 wt% dodecane and 70 wt% bitumen, and distilled water were used in the trial. Core was left in vacuum pump for two hours in oven before it was put into the Amott cell.

Trial 10

Trial 10 was the last trial in the optimization process due to the time span of present thesis. In this trial a lower viscosity of the heavy oil was used than in the

previous nine trials. The heavy oil mixture was of 66 wt% bitumen, and had a viscosity of 20 cp at 60 °C. The core holder was filled with glass beads of 425 – 600 μm. Unsuccessful as no oil came out of the core after one week in the oven at 60 °C.

FIGURE B.9: Trial 10, IMBIBITION: artificial core made of 425 – 600 μm glass beads and small steel filter. 60 °C in oven. Heavy oil mixture of 34 wt% dodecane and 66 wt% bitumen, and distilled water were used in the trial. Core was left in vacuum pump for two hours in oven before it was put into the Amott cell. Still some observed problems with air at filter.

C | Results From Measurements of Core and Fluid Properties

C.1 Permeability Measurements

Table C.1 is the measurement of porosity for the two cores permeability was measured on. The porosity for the cores used in the spontaneous imbibition test are given in Appendic D.

TABLE C.1: Results from porosity measurement before permeability measurement.

Core #	L mm	V_b [cm^3]	V_1 [cm^3]	V_2 [cm^3]	V_{gb} [cm^3]	ϕ [%]	V_p [cm^3]
A	51.8	38.0	72	29.8	24.2	0.363	13.77831
B	51.7	37.8	72	29.7	24.3	0.358	13.53304

TABLE C.2: Results from the permeability measurement of core A.

Diameter [cm]	3.4	Q atm	Q atm	Δ P	Δ P	k
Areal [cm^2]	9.08	[mL/min]	[cm^3/s]	[mbar]	[bar]	[D]
Length [cm]	5.183	5.1	0.085	4.6	0.0046	10.549
my [cp]	1	10.2	0.170	12.2	0.0122	7.955
(my * L) / A	0.571	2	0.033	1.9	0.0019	10.015
		3.1	0.052	2.95	0.0030	9.998

TABLE C.3: Results from the permeability measurement of core B.

Diameter [cm]	3.4	Q atm	Q atm	Δ P	Δ P	k
Areal [cm^2]	9.08	[mL/min]	[m^3/s]	[mbar]	[Pa]	[D]
Length [cm]	5.167	5.1	0.085	6.6	0.0066	7.33
my [cp]	1	3	0.050	2.7	0.0027	10.54
(my * L) / A	0.569	2	0.033	1.2	0.0012	15.81

C.2 Nanofluids Properties

The density (Table C.5) and viscosity (Table C.6) of the nanofluids used in the surface coating of the glass beads for the imbibition tests was measured on the mixtures shown in Table C.4.

TABLE C.4: Nanofluid preparation, weights and checking the weight percentages.

	Base fluid	NP	
	gr	gr	wt %
Hydrophilic 0.01 wt%	299.97	0.030	0.010
Hydrophilic 0.1 wt%	299.7	0.305	0.102
Hydrophilic 0.5 wt%	298.52	1.503	0.501
Hydrophobic NR 0.01 wt%	299.97	0.031	0.010
Hydrophobic NR 0.1 wt%	299.7	0.299	0.100
Hydrophobic NR 0.5 wt%	298.5	1.500	0.500

TABLE C.5: The density of heavy oil, nanofluids and distilled water where measured with a picknometer of 25 mL. The room temperature was 21.8 at the time of measurement.

Fluid	liquid (g)	Picnometer volume (cm^3)	Denisty ρ (g/cm^3)
Heavy oil	22.38	25	0.895
Distilled water	24.989	25	0.99956
Hydrophilic 0.01 wt%	24.979	25	0.99916
Hydrophilic 0.1 wt%	25.003	25	1.00012
Hydrophilic 0.5 wt%	25.47	25	1.0188
Hydrophobic NR 0.01 wt%	19.741	25	0.78964
Hydrophobic NR 0.1 wt%	19.751	25	0.79004
Hydrophobic NR 0.5 wt%	19.79	25	0.7916

TABLE C.6: Viscosity was determined with the use of a capillary viscometer. Poiseuille law (Equation 3.2) was used to calculate viscosity from the travel time recorded. H.philic: Hydrophilic.

k_1	0.001980	mm^2/s^2					
k_2	0.001635	mm^2/s^2					
Fluid	t_1 [s]	t_2 [s]	t_3 [s]	υ_1	υ_2	υ_{av}	μ
Di water	287	780	1371	0.976	0.966	0.971	0.970
H.philic 0.01 wt%	396	883	1474	0.964	0.966	0.965	0.964
H.philic 0.01 wt%	458	947	1538	0.968	0.966	0.967	0.967
H.philic 0.1 wt%	176	661	1246	0.960	0.956	0.958	0.959
H.philic 0.5 wt%	265	800	1451	1.059	1.064	1.062	1.082

D Results From to the Spontaneous Imbibition Test

In the present appendix the rates recorded during the experiment and pictures of the Amott cells at the end of the spontaneous imbibition test is given. The results from the porosity measurements on all the cores used in the imbibition testing are also given. For the tables with results from the porosity measurements: V1 is the reference volume of the cell before core holder with glass beads is placed. V2 is the volume of cell with holder, filter and glass beads. Vgb is the volume of the glass beads. Vgb = V1 - V2 - Vh where Vh is the volume of the core holder and filters.

D.1 Preparation of Glass Beads

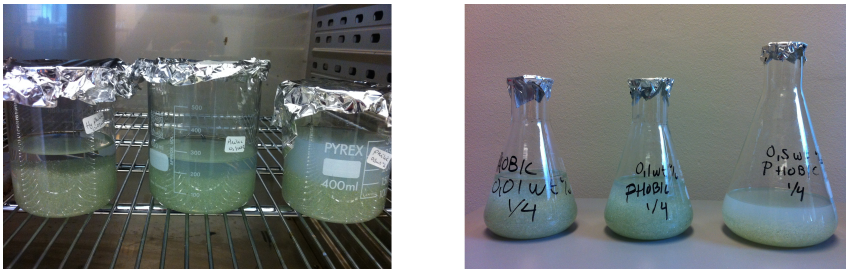

FIGURE D.1: Glass beads of 1 mm submerged in nanofluids. From the left: Hydrophilic 0.01 wt%, hydrophilic 0.1 wt%, hydrophilic0.5 wt%, hydrophobic 0.01 wt%, hydrophobic 0.1 wt% and hydrophobic 0.5 wt%.

D.2 Initial Experiments

TABLE D.1: Porosity measurements of the prepared cores.

Core #	L mm	V_b [cm^3]	V_1 [cm^3]	V_2 [cm^3]	V_{gb} [cm^3]	ϕ [%]	V_p [cm^3]	V_{end} [cm^3]
A	52.1	38.2	72	29.6	24.4	0.362	13.8	11.6
B	51	37.2	72	29.9	24.1	0.353	13.1	10.9
C	52.7	38.8	73	29.5	25.5	0.342	13.3	13
D	52.2	38.3	73	29.4	25.6	0.332	12.7	12.7

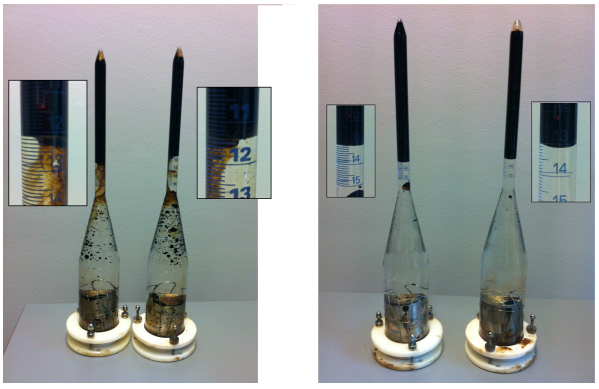

FIGURE D.2: Amott cells with core A, B, C and D from the left. The cores are all made of none treated glass beads.

TABLE D.2: Data from imbibition method with none surface treated cores.

Core A		Core B		Core C		Core D	
Time	Vs [mL]	Time	Vs [mL]	Time	Vs [mL]	Time	Vs [mL]
00:05:56	0	00:04:53	0	00:14:04	0.3	00:06:20	0.6
00:05:56	1.5	00:04:53	0.6	00:15:54	0.80	00:07:28	1
00:07:38	2.7	00:09:37	3.2	00:17:56	1.30	00:07:55	1.3
00:08:20	3.5	00:24:34	8.1	00:19:45	1.80	00:09:50	1.6
00:08:53	3.9	00:30:07	9	00:21:40	2.30	00:10:04	2.1
00:09:31	4.3	00:34:11	9.7	00:23:35	2.90	00:11:51	2.4
00:12:36	6.1	00:42:39	10.4	00:25:12	3.40	00:12:33	2.8
00:27:52	10.9	01:31:00	11	00:26:49	3.90	00:13:58	3.3
01:31:00	11.7			00:28:23	4.40	00:15:06	3.7
				00:29:42	4.90	00:17:06	4.3
				00:31:01	5.30	00:19:05	4.8
				00:32:20	5.8	00:20:50	5.6
				00:33:39	6.2	00:22:30	6
				00:34:58	6.7	00:24:09	6.4
				00:37:58	7.9	00:26:10	6.7
				00:40:58	8.3	00:28:12	6.7
				00:43:40	9	00:30:59	7.1
				00:46:22	9.4	00:34:02	7.4
				00:55:00	10.9	00:37:05	7.9
				01:00:18	11.3	00:39:30	8.3
				01:08:50	11.7	00:42:50	8.7
				01:11:22	12	00:46:10	9.1
						00:53:07	9.5
						00:53:37	9.9
						01:00:38	10.2
						01:02:38	10.7
						01:19:02	11.5

D.3 Hydrophilic Experiments

TABLE D.3: Porosity measurements and results for the imbibition test of the hydrophilic 0.01 wt% cores.

Core #	L mm	V_b [cm^3]	V_1 [cm^3]	V_2 [cm^3]	V_{gb} [cm^3]	ϕ [%]	V_p [cm^3]	V_{end} [cm^3]
A	52	38.1	72	29.6	24.4	0.360	13.7	13.3
B	52	38.1	72	29.4	24.6	0.355	13.5	10.7

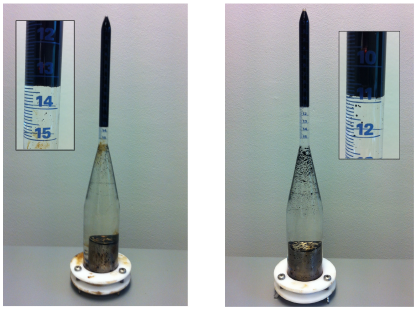

FIGURE D.3: Artificial core made of glass beads soaked in 0.01 wt % hydrophilic nanofluid. Core A is to the left and core B is to the right.

FIGURE D.4: Artificial core made of glass beads soaked in 0.1 wt % hydrophilic nanofluid. From left: Core A, B and C.

TABLE D.4: Data from imbibition method with cores of hydrophilic 0.01 wt% treated glass beads.

Core A		Core B	
Time	Vs [mL]	Time	Vs [mL]
00:02:00	0.2	00:00:22	0.6
00:02:30	0.9	00:00:52	1.1
00:03:40	1.6	00:01:18	1.9
00:04:40	2.1	00:01:44	2.6
00:05:50	2.7	00:02:09	3.2
00:06:20	3.3	00:02:35	3.8
00:07:24	3.9	00:03:02	4.4
00:08:35	4.5	00:03:30	5.1
00:09:55	5.2	00:03:57	5.7
00:11:17	5.8	00:04:23	6.4
00:13:10	6.5	00:04:58	7.1
00:14:23	7	00:05:24	7.8
00:15:45	7.6	00:05:57	8.4
00:17:29	7.9	00:06:30	9.1
00:19:20	8.6	00:07:06	9.8
00:21:40	9	00:07:56	10.5
00:23:17	9.3	00:08:39	11.1
00:27:38	9.8	00:09:43	11.7
01:00:00	10.7	01:00:00	12.2

TABLE D.5: Porosity measurements and results for the imbibition test of the hydrophilic 0.1 wt% cores. Core A went out of scale.

Core #	L mm	V_b [cm^3]	V_1 [cm^3]	V_2 [cm^3]	V_{gb} [cm^3]	ϕ [%]	V_p [cm^3]	V_{end} [cm^3]
A	51	37.2	72	30.2	23.8	0.361	13.4	$\sim$
B	51	37.2	72	30	24	0.355	13.2	10.3
C	52	38.1	72	29.6	24.4	0.360	13.7	12.3

TABLE D.6: Data from imbibition method with cores of hydrophilic 0.1 wt% treated glass beads.

Core A		Core B		Core C	
Time	Vs [mL]	Time	Vs [mL]	Time	Vs [mL]
00:07:00	3.00	00:02:00	1.4	00:09:27	0.5
00:09:00	4.10	00:04:00	3.2	00:12:07	1.2
00:11:00	6.70	00:06:00	4.3	00:16:20	1.7
00:13:00	6.70	00:13:00	7.2	00:18:25	2.25
00:20:00	9.00	00:25:00	9.5	00:20:26	2.8
00:32:00	9.50	00:28:00	9.9	00:22:18	3.3
00:35:00	9.50	00:35:00	9.9	00:22:39	3.9
00:42:00	9.50	00:50:00	10.2	00:24:50	4.5
00:57:00	10.00	01:32:00	10.5	00:27:14	5.1
01:39:00	10.00	01:58:00	10.6	00:29:59	5.7
02:05:00	10.00			00:33:11	6.3
				00:35:06	6.8
				00:36:23	8
				00:45:23	8.7
				00:52:18	9.4
				01:01:09	9.9
				01:13:38	10.5
				01:14:54	11
				01:39:13	11.1

TABLE D.7: Porosity measurements and results for the imbibition test of the hydrophilic 0.5 wt% cores. End volume for core C was approximated because the improper cleaning lead to blockage of inlet to measuring tube.

Core #	L mm	V_b [cm^3]	V_1 [cm^3]	V_2 [cm^3]	V_{gb} [cm^3]	ϕ [%]	V_p [cm^3]	V_{end} [cm^3]
A	52	38.1	72	29.7	24.3	0.363	13.8	-
B	51	37.2	72	30.2	23.8	0.361	13.4	~ 12
C	52	38.1	72	29.7	24.3	0.363	13.8	~ 9
D	52.2	38.3	72	29.9	24.1	0.371	14.2	6

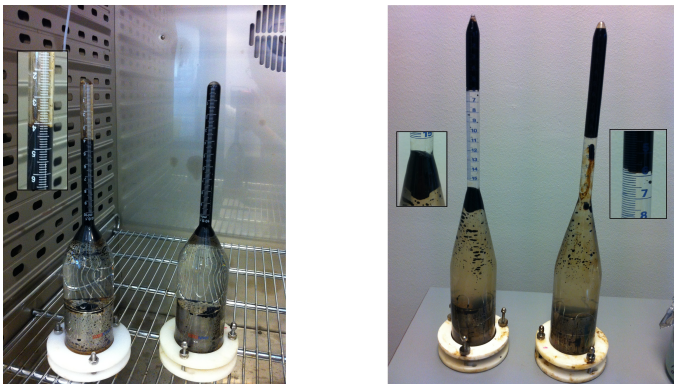

FIGURE D.5: Artificial core made of glass beads soaked in 0.5 wt % hydrophilic nanofluid. From left: Core A, B, C and D.

TABLE D.8: Data from imbibition method with cores of hydrophilic 0.5 wt% treated glass beads.

Core A		Core B		Core C		Core D	
Time	Vs [mL]	Time	Vs [mL]	Time	Vs [mL]	Time	Vs [mL]
00:16:00	6.6	00:11:00	6.7	00:08:18	0.5	00:06	0
00:23:00	8.6	00:18:00	10.5	00:10:35	0.9	00:23	0.4
00:29:00	9.6	00:24:00	11.5	00:13:51	1.3	00:28	0.9
00:35:00	10.2	00:30:00	12	00:15:30	1.8	00:32	1.3
00:41:00	10.5	00:36:00	12	00:19:14	2.3	00:37	1.7
00:46:00	11	00:41:00	12.5	00:25:00	2.8	00:44	2.4
00:50:00	11.5	00:45:00	12.5	00:32:49	3.4	00:49	2.8
01:10:00	11.5	01:05:00	12.5	00:41:33	4	00:55	3.5
01:38:00	11.5	01:33:00	13	00:51:22	4.6	01:01	3.9
				00:57:51	5.50	01:08	4.8
				01:11:37	5.5	01:17	5.2

D.4 Hydrophobic Experiments

TABLE D.9: Porosity measurements and results for the imbibition test of the hydrophobic 0.01 wt% cores.

Core #	L mm	V_b [cm^3]	V_1 [cm^3]	V_2 [cm^3]	V_{gb} [cm^3]	ϕ [%]	V_p [cm^3]	V_{end} [cm^3]
A	52	38.1	72	29.2	24.8	0.350	13.3	12.5
B	51	37.2	72	29.2	24.8	0.334	12.4	12.1

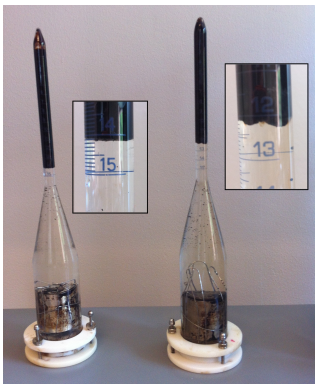

FIGURE D.6: Artificial core made of glass beads soaked in 0.01 wt % hydrophobic nanofluid. Core A is to the left and core B is to the right.

TABLE D.10: Porosity measurements and results for the imbibition test of the hydrophobic 0.1 wt% cores.

Core #	L mm	V_b [cm^3]	V_1 [cm^3]	V_2 [cm^3]	V_{gb} [cm^3]	ϕ [%]	V_p [cm^3]	V_{end} [cm^3]
A	52	38.1	72	29.4	24.6	0.355	13.5	-
B	52	38.1	72	30.2	23.8	0.376	14.3	13.3
C	51	37.2	73	30.6	24.4	0.345	12.8	-
D	51.5	37.7	72	29.9	24.1	0.361	13.6	12.1
E	52.9	38.9	72	29.5	24.5	0.371	14.4	12.0

FIGURE D.7: Artificial core made of glass beads soaked in 0.1 wt % hydrophobic nanofluid. The picture is of Core B. No pictures was taken for Core A and Core C. Core A was aborted due to improper cleaning of Amott cell. For Core C no oil came out. Core was left saturated in heavy oil for 2 days.

TABLE D.11: Data from imbibition method with cores of hydrophilic 0.5 wt% treated glass beads.

Core A 0.01 wt%		Core B 0.01 wt%		Core B 0.1 wt%	
Time	Vs [mL]	Time	Vs [mL]	Time	Vs [mL]
00:04:30	0	00:02:04	0.2	0.0233	0
00:05:12	0.8	00:03:30	0.6	0.0233	0.8
00:05:55	1	00:04:16	0.95	0.0273	1.3
00:06:40	1.5	00:05:00	1.3	0.0301	1.9
00:07:23	1.7	00:05:45	1.6	0.0339	2.5
00:08:11	2	00:06:22	2	0.0385	3.1
00:08:16	2.3	00:06:59	2.4	0.0417	3.8
00:08:57	2.7	00:07:36	2.8	0.046	4.4
00:09:42	3	00:08:13	3.2	0.0508	5
00:10:04	3.3	00:08:52	3.55	0.0563	5.7
00:10:30	3.5	00:09:30	3.9	0.0621	6.3
00:11:16	3.8	00:10:10	4.3	0.0684	6.9
00:12:09	4.5	00:10:49	4.7	0.0751	7.45
00:12:55	4.8	00:11:32	5.1	0.082	8.2
00:14:37	5.8	00:12:17	5.5	0.089	8.75
00:15:30	6	00:13:05	5.9	0.1013	9.3
00:16:23	6.7	00:13:55	6.3	0.1031	9.9
00:17:16	7	00:14:49	6.7	0.1552	12.2
00:18:10	7.3	00:15:48	7		
00:19:13	7.9	00:16:51	7.4		
00:20:16	8.1	00:17:58	7.8		
00:22:29	8.9	00:19:14	8.15		
00:23:18	9.4	00:20:44	8.5		
00:23:47	9.6	00:22:31	8.85		
00:25:03	9.9	00:24:40	9.3		
00:27:23	10.5	00:30:28	9.9		
00:29:53	10.9	00:35:46	10.3		
00:31:44	11.2	00:37:52	10.8		
02:03:00	12.1	01:04:30	11.25		

TABLE D.12: Porosity measurements and results for the imbibition test of the hydrophobic 0.5 wt% cores. No significant amount of oil came out for any of the cores.

Core #	L mm	V_b [cm^3]	V_1 [cm^3]	V_2 [cm^3]	V_{gb} [cm^3]	ϕ [%]	V_p [cm^3]	V_{end} [cm^3]
A	51.5	37.7	72	30.6	23.4	0.379	14.3	1.2
B	52	38.1	72	30	24	0.371	14.1	0.2
C	51.7	37.9	72	30.2	23.8	0.371	14.1	0

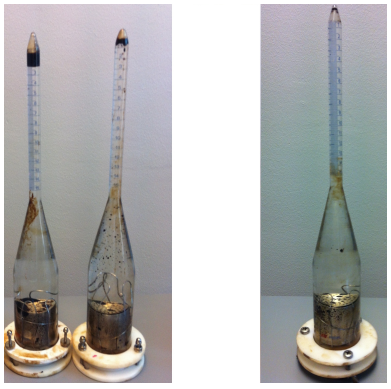

FIGURE D.8: Artificial core made of glass beads soaked in 0.5 wt % hydrophobic nanofluid. From the left: Core A, B and C. No significant amount of oil came out for any of the cores.

E | Results from Contact Angle Measurements

The results from the contact angle and interfacial tension measurements are shown as graphs below. The weights of the prepared nanofluids are shown in Table E.1.

TABLE E.1: Preparation of the nanofluids used in the contact angle and interfacial tension measurements.

	Base fluid	NP	
	gr	gr	wt %
Hydrophilic 0.01 wt%	199.98	0.02087	0.010
Hydrophilic 0.1 wt%	299.72	0.302	0.101
Hydrophilic 0.5 wt%	298.5	1.499	0.500

The measurments from the imaging method is plotted in Figure E.1, Figure E.2, Figure E.3 and Figure E.4. It was determined to only include the plots in this appendix due to the large volume of data, and the data is better understood as a plot.

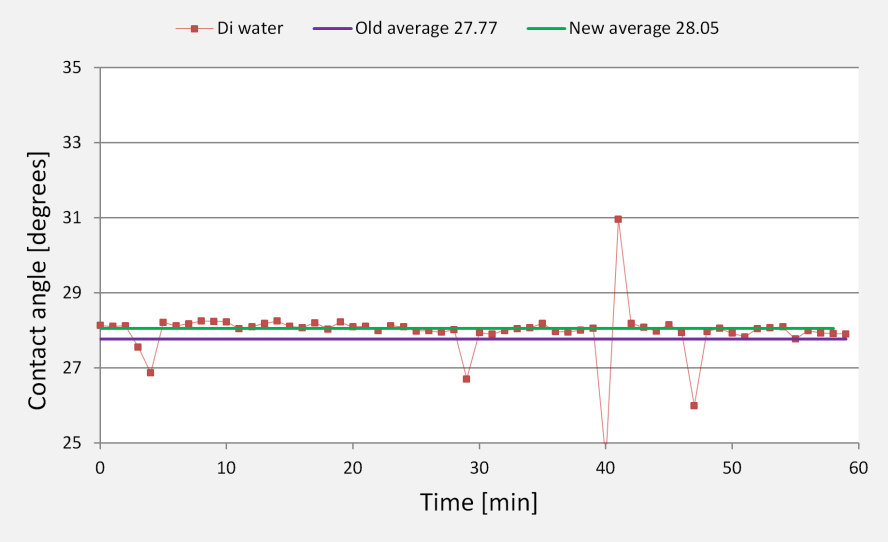

FIGURE E.1: Interfacial tension measurement of a heavy oil droplet in di water.

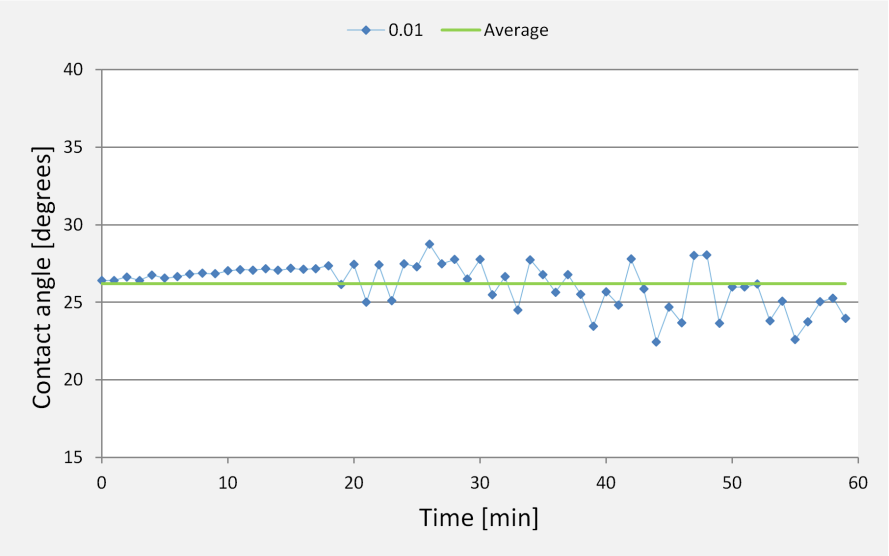

FIGURE E.2: Interfacial tension measurement of a heavy oil droplet in 0.01 wt% hydrophilic nanofluid.

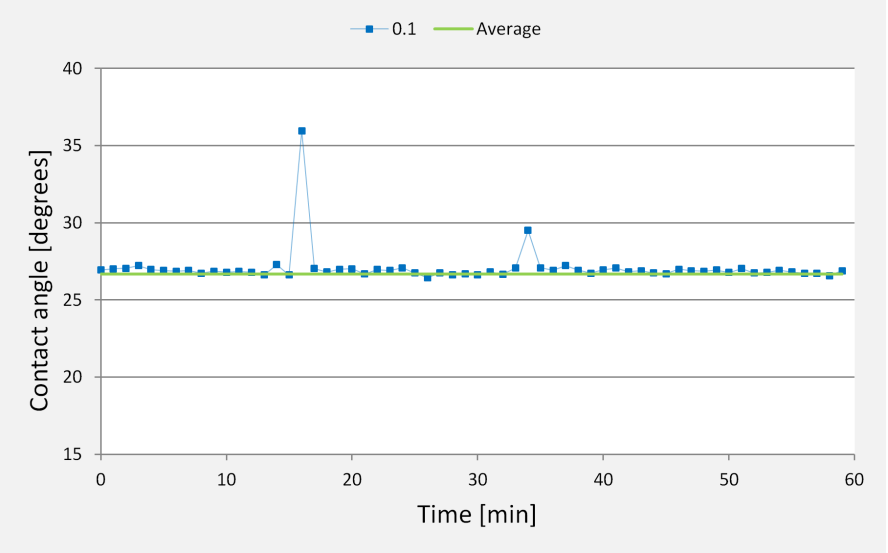

FIGURE E.3: Interfacial tension measurement of a heavy oil droplet in 0.1 wt% hydrophilic nanofluid.

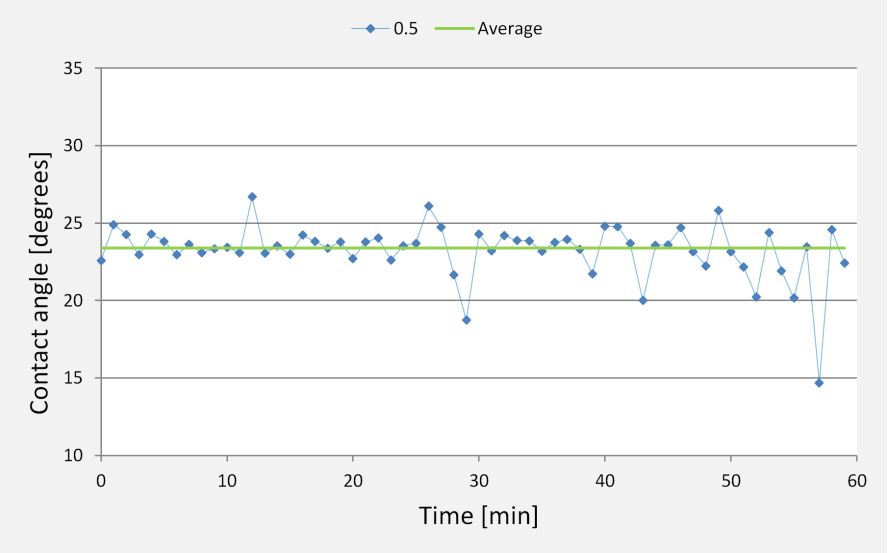

FIGURE E.4: Interfacial tension measurement of a heavy oil droplet in 0.5 wt% hydrophilic nanofluid.

F Results From Interfacial Tension Measurement

The measurments from the spinning drop method is plotted in Figure F.1, Figure F.2, Figure F.3 and Figure F.4. It was determined to only include the plots in this appendix due to the large volume of data. For each experiment it took about 3-4 hours for the system to reach equilibrium. Equilibrium is reached when the measurement is stabilized. The experiments were ended when the measured value of the interfacial tension had been stable for at least 15 min.

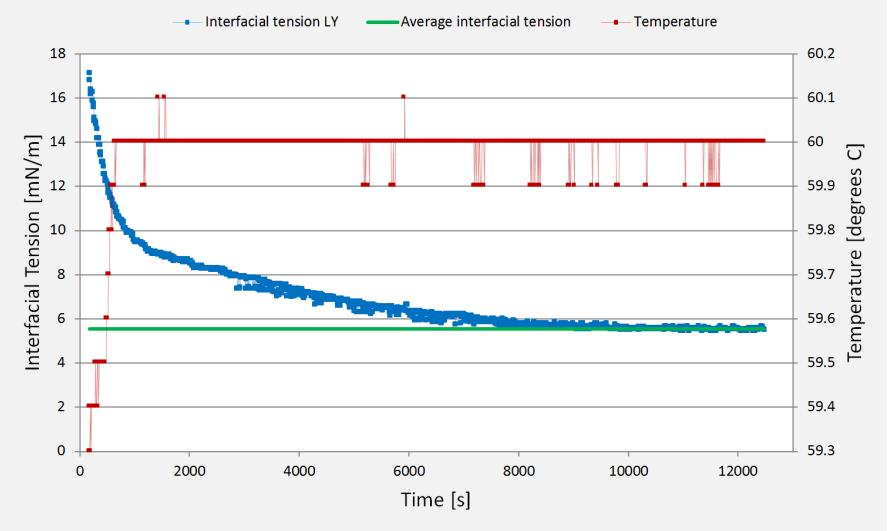

FIGURE F.1: Interfacial tension measurement of a heavy oil droplet in distilled water.

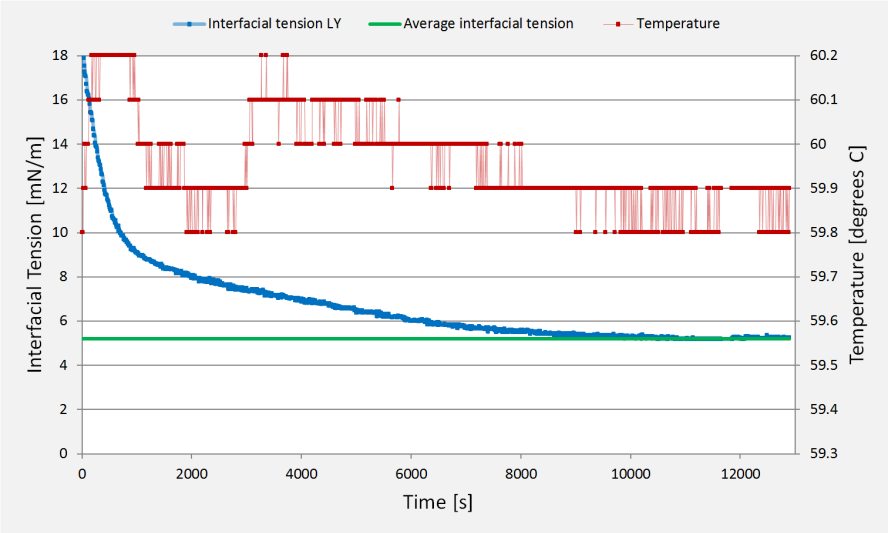

FIGURE F.2: Interfacial tension measurement of a heavy oil droplet in nanofluid with 0.01 wt% silica nanoparticles.

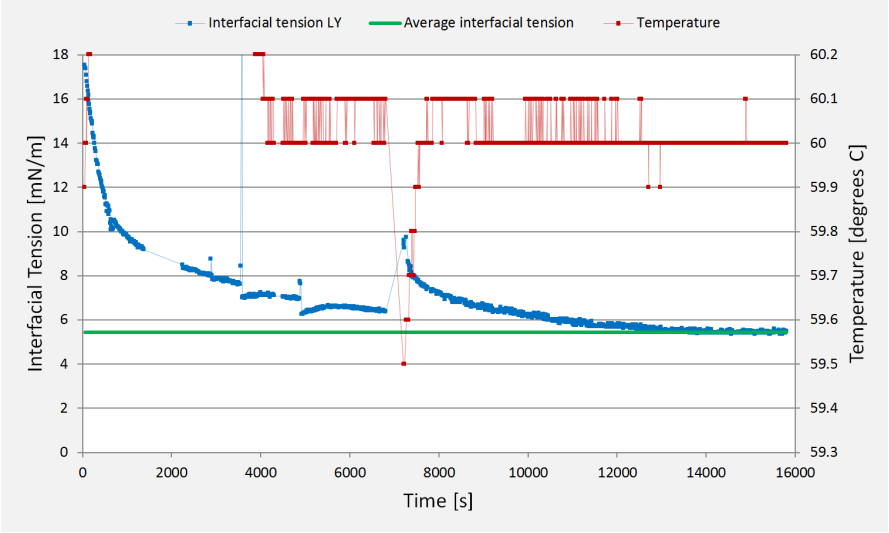

FIGURE F.3: Interfacial tension measurement of a heavy oil droplet in nanofluid with 0.1 wt% silica nanoparticles.

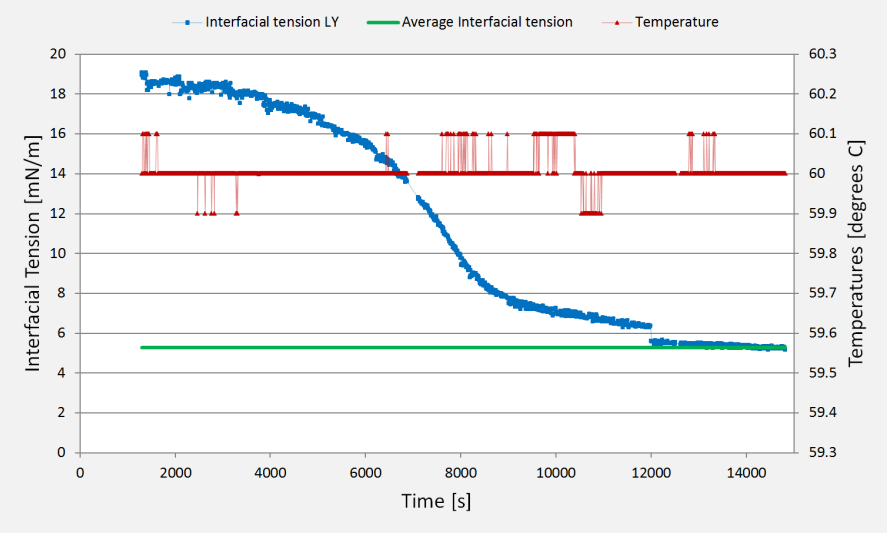

FIGURE F.4: Interfacial tension measurement of a heavy oil droplet in nanofluid with 0.5 wt% silica nanoparticles.